



## GEOLOGICAL SURVEY OF CANADA

OPEN FILE 1788

---

### A Summary of the 2001 Sable Island Bank Hydrodynamic and Bedform Data

---

C. Smyth , M. Li and D. Heffler

2003

**GEOLOGICAL SURVEY OF CANADA**

**OPEN FILE 1788**

**A summary of the 2001 Sable  
Island Bank Hydrodynamic and Bedform Data**

**C. Smyth, M. Li, and D. Heffler**

**2003**

©Her Majesty the Queen in Right of Canada 2003  
Available from  
Geological Survey of Canada  
1 Challenger Drive  
Dartmouth, Nova Scotia B2Y 4A2

**Smyth, C., Li, M., and Heffler, D.**  
**2003:** A summary of the 2001 Sable Island Bank Hydrodynamic and Bedform Data,  
Geological Survey of Canada, Open File 1788, 45 p.

Open files are products that have not gone through the GSC formal publication process.

## Contents

<b>1</b>	<b>Introduction</b>	<b>2</b>
<b>2</b>	<b>Experiment Summary</b>	<b>2</b>
2.1	Instrument Location . . . . .	2
2.2	Instrumentation . . . . .	2
2.3	Hydrodynamic Observations . . . . .	4
2.4	Bedforms . . . . .	7
2.5	Mobile Layer Depth . . . . .	9
2.6	Sediment Suspension . . . . .	11
<b>3</b>	<b>Predictions by SEDTRANS96</b>	<b>11</b>
<b>4</b>	<b>Acknowledgments</b>	<b>12</b>
<b>A</b>	<b>Tidal Analysis</b>	<b>13</b>
<b>B</b>	<b>SEDTRANS96 inputs and predictions</b>	<b>14</b>

## 1 Introduction

A joint project between the Geological Survey of Canada and the Sable Offshore Energy Project was initiated in 1995 to monitor wave-current dynamics and seabed responses during storms on the Scotian Shelf. One of the goals of this project is to investigate the interaction between bottom boundary layer dynamics and sediment transport. In order to reach this goal, detailed measurements of flow dynamics and sediment transport modes have been collected.

This report summarizes the 2001 experiment which deployed instrumented frames approximately 30 km west of Sable Island at the Cohasset-Panuke (CoPan) site. Measurements include wave and current velocities, acoustic seafloor images, and suspended sediment profiles. These measurements are analyzed to determine the mobile layer depth and the magnitude and direction of sediment transport during storm conditions. Detailed scientific interpretations of these data will be presented in subsequent scientific publications.

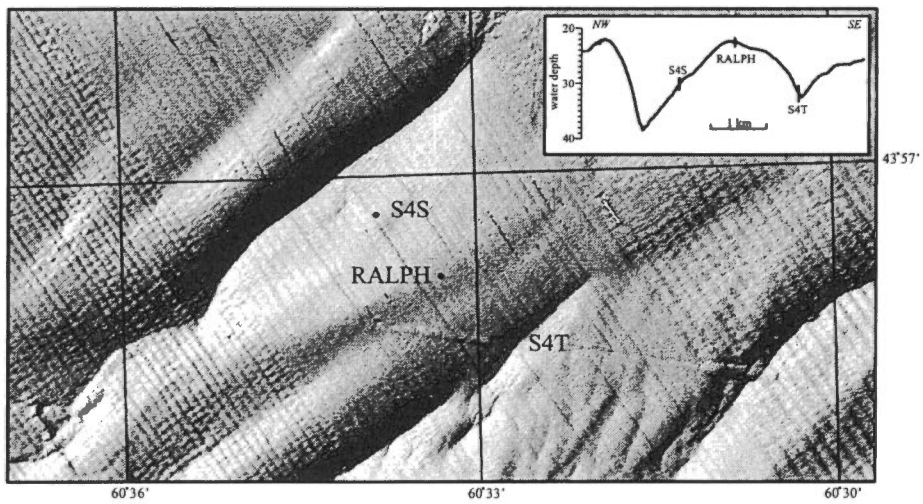
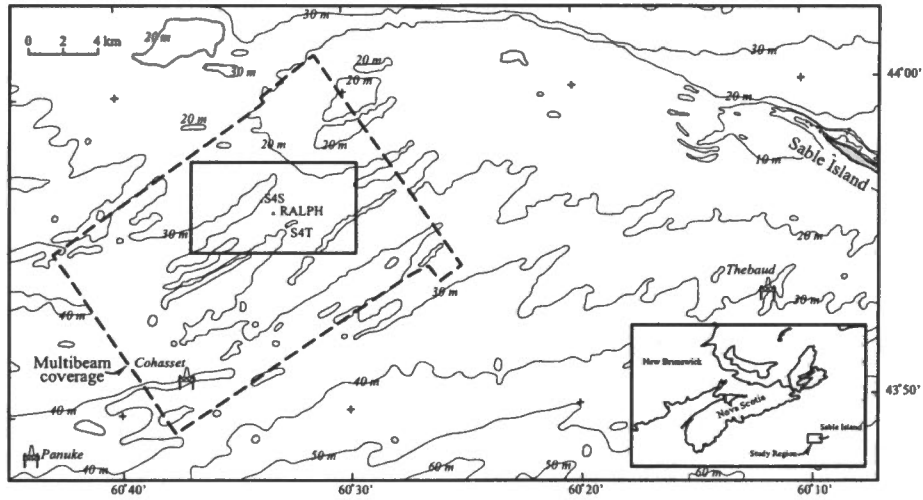
## 2 Experiment Summary

### 2.1 Instrument Location

Three frames were deployed along a sand-ridge transect at a CoPan site on January 15th, 2001, including two S4 current meter frames, and an autonomous quad frame called Ralph. Ralph was positioned on the crest of a O(10 m) high sand ridge in 23 m water depth (Figure 1). The two S4 frames were placed on either side of Ralph along the transect of the sand ridge with the first frame (S4S) to the northwest of Ralph on the ridge slope in 32 m water depth, and the second frame (S4T) approximately 1 km to the southeast of Ralph in the trough. Frame locations are given in Table 1.

### 2.2 Instrumentation

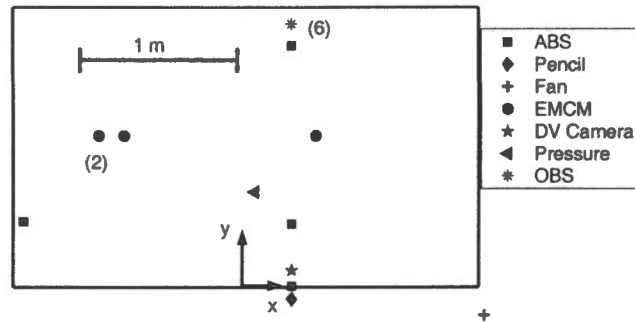
Instruments on Ralph estimate water depth, wave and current velocity, suspended sediment levels, and record bedform images. Table 2 briefly summarizes the instrumentation on Ralph, but a more thorough description is given by *Heffler* [1996]. Six computers were used to control instruments, including 2 Tattletale 5F's, 3



SIB/illustrations/CoPan Ralph index map.cdr

Figure 1: Top panel: location of the Ralph instrument frame and two S4 current meters are shown along with Sable Island Bank bathymetry. Bottom panel: expanded inset region showing shaded relief image from multibeam bathymetry indicating the sand ridges. The illumination direction is 135°, measured clockwise from north. Inset: transect profile indicating the location of Ralph frame on the crest, one S4 frame in the trough, and a second S4 on the stoss slope.

Figure 2: Plan view of the Ralph frame showing instrument locations.



Tattletale 7's and 1 Compact Flash 1. Data were stored on 3 hard drives (a total of 1.5 Gb), and an additional 22 Gb camera tape. Instrument positions on the frame are given with respect to a reference origin, Figure 2.

Two InterOcean S4 current meters measured pressure, wave and current velocity, compass direction and optical backscatter amplitude. Each S4 sensor was mounted on an aluminum tubular frame 50 cm above the bed with an additional OBS sensor adjacent to the S4 at a height of 70 cm. The sampling frequency, burst duration and burst interval for all of the instruments is given in Table 3. S4T failed to record any data.

Surficial sediment samples from 2 van Veen grab samples were collected at each frame location. Median grain diameters were 411  $\mu\text{m}$  at Ralph's location and 493  $\mu\text{m}$  at the S4S frame location.

### 2.3 Hydrodynamic Observations

Ralph was deployed on the crest of a sand ridge at the CoPan site. The S4S frame was deployed roughly half-way down the stoss (western) flank of the sand ridge. The mean current speed and significant wave height recorded respectively by the S4 and Ralph are plotted in Figure 3 as a function of time. The mean current for was measured at approximately 70 cm above the seabed on the Ralph frame, and at approximately 50 cm for the S4. Though the lower measurement height could slightly reduce the mean current recorded by the S4 meter, the average difference should be <10%.

Eight events passed the area in this deployment (Figure 3b). Two significant storms, with significant wave heights at the surface,  $H_s$ , of approximately 4 m, occurred on yeardays 22 and 31 respectively. There were six minor storms in which  $H_s$  reached around 2 m. Surface significant wave heights were corrected for depth attenuation of higher frequency wave energy. An energy threshold was applied at high frequencies to prevent noise attenuation. The noise threshold was assumed to be half of the precision of the pressure data, identified as  $\pm 15\%$  of the full scale depth (70 m).

Figure 3c shows the time series of the water depth at the Ralph site. Spring tide occurred in the middle part of the deployment and tidal range was approximately 1.1 m in this period. Neap tides occurred at the beginning and end of the deployment, in which the tidal range was as low as 0.7 m. The inequality of the

Table 1: Instrument frame locations for the 2001 deployment. The instruments are abbreviated as follows: EMCM, Electro-magnetic Current Meter; OBS, Optical Backscatter Sensor; ABS, Acoustic Backscatter Sensor; and DV Camera, Digital Video Camera.

Frame	Instruments	Latitude	Longitude
S4S	S4, OBS (S/N 1590)	43° 56.6' N	60° 33.7' W
S4T	S4 (S/N 2196)	43° 55.8' N	60° 32.6' W
Ralph	6 OBS, Pressure, Tilt, Temperature, 4 EMCM, 4 ABS, Compass, DV Camera	43° 56.3' N	60° 33.2' W

Table 2: Instrument descriptions and positions on the Ralph frame

Sensor	Variable Measured	Brand	Position (X,Y,Z) [cm]	Computer and Drive
Pressure Sensor	water depth	Data Inst. Model AB	12,90,150	TT7 120 Mb
Compass/Tilt	dir/tilt/temp	Precision Nav. TCM2	22,90,150	TT7 120 Mb
4 EMCM's	fluid velocity	Marsh McBirney	-88,137,30 50,137,50 -72,137,70 -88,137,100	TT5F 120 Mb
6 OBS	suspended sediment	SeaPoint Inst., 125 FTU	35,220,10 35,220,30 35,220,50 35,220,70 35,220,100 35,220,175	CF1 120 Mb
4 ABS	seafloor elevation suspended sediment profile	Mesotech, 1 MHz	35,11,132 35,65,132 35,212,132 -136,63,132	TT7 540 Mb
Pencil beam	bedform size	Imagenex 881P, 0.675 MHz	35,0,132	TT7 840 Mb
Fan beam	bedform size/type	Imagenex 881I, 0.675 MHz	156,-14,158	TT7
DV Camera	sed. motion	Sony EX1000	35,24,132	TT5 90 min
Relocation Fingerprint		Vemco		

Table 3: Burst information for the instrumentation

Instrument	Sampling Frequency [Hz]	Burst Duration [min]	Interval between Bursts [hrs]	Start time [min:s]
Pressure, Compass, OBS, EMCM	5	14	2	00:01
ABS	1	1	2	00:03
Pencil beam	1 image/burst	1.5	2	00:08
Fan beam	1 image/burst	2.3	2	01:38
S4S	2	10	2	18:00
OBS (with S4S)	1	10	1	00:01

mixed semi-diurnal tide on Sable Island Bank is apparent in Figure 3c. A larger tide range is generally followed by a smaller tidal range in the next cycle (see also Appendix A).

The comparison of mean velocity in Figure 3a shows that the mean current speed over the sand ridge crest is much higher than that on the stoss flank; peak mean current speeds on the crest reached more than 0.7 m/s while that on the mid-stoss were approximately 0.4 m/s. In agreement with *Li et al.* [1999], this data set shows that the mean current was likely suppressed at the peaks of storms (e.g. yeardays 22 and 30). The across-ridge variation of mean current speed and direction and possible causes are further explored by comparing the mean current speed and its direction for individual storms in Figures 4 and 5.

The time series of mean current direction and speed, and significant wave height recorded by Ralph and S4S for storms on yeardays 20 to 24 is shown in Figure 4. Since the direction of peak mean current is often in the first and fourth quadrants, a value of 360° was added to the mean current directions that were less than 45°. Figures 4a and 4b show that the peak mean currents were generally enhanced from about 0.4 m/s at the

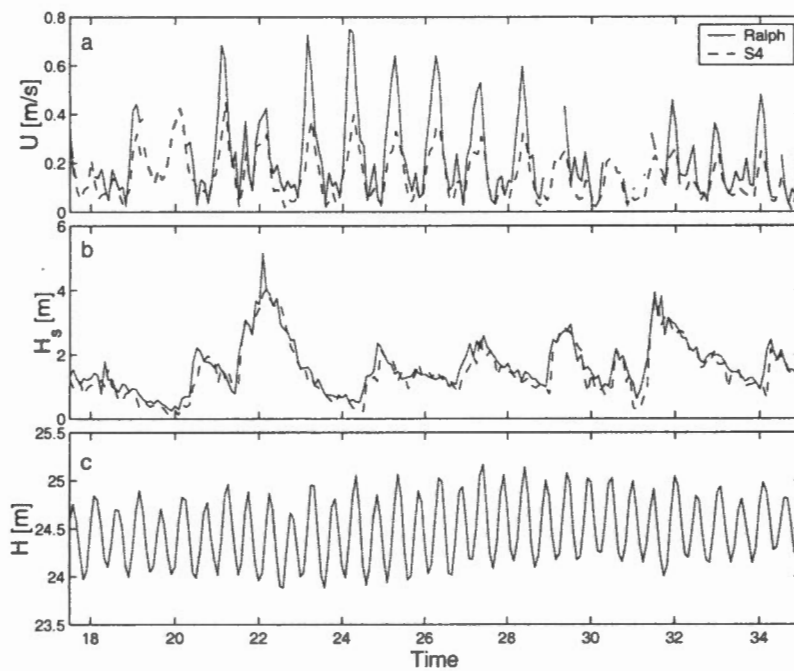


Figure 3: Time series of: (a) average current magnitude,  $U$ , measured by the EMC M current meter on Ralph and the S4 current meter, (b) significant wave height corrected for depth attenuation and (c) water depth.

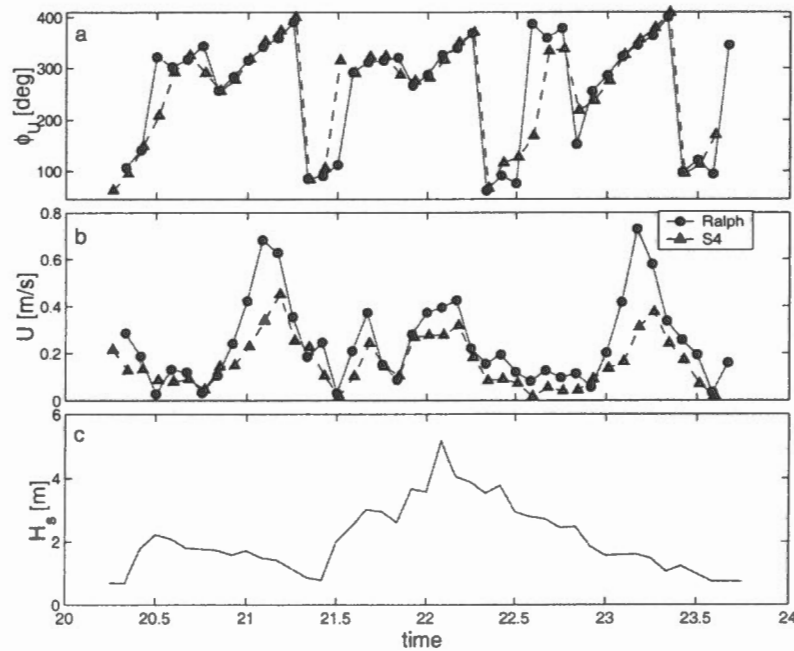


Figure 4: Time series of: (a) average current direction measured for the Ralph and S4 frames, (b) average current magnitude and (c) surface significant wave height for the storm on yearday 22.

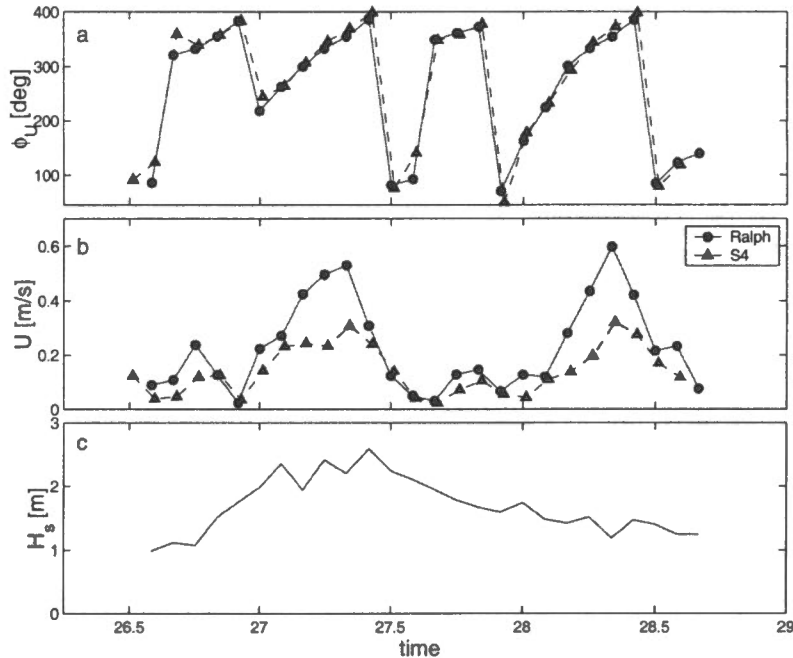


Figure 5: Time series of: (a) average current direction measured for the Ralph and S4 frames, (b) average current magnitude and (c) surface significant wave height.

mid-stoss to about 0.7 m/s over the ridge crest. The direction of the peak mean current is to the N and NNW and is similar for the crest and stoss side, though the mean current on the ridge crest lagged (approximately  $30^\circ$ ) behind that of the mid-stoss in the clockwise rotation. Comparing the mean current speed and the significant wave height (Figures 4b and 4c) shows that two main peaks of mean current occurred during storm spin downs. In contrast, at the peak of the storm on yearday 22, where  $H_s$  reached about 5 m, strong wind-driven current offset the tidal current so that the total mean current was suppressed to about 0.4 m/s over the sand-ridge crest.

The same current and wave parameters for the storm on yearday 27 are plotted in Figure 5. Two peaks of mean current occurred during this storm: one over the peak of the storm and the second one during the gradual spin-down of the storm. Again the maximum mean current was much stronger on the sand ridge crest than that on the stoss side, 0.5 - 0.6 m/s versus 0.3 m/s. The direction of the peak mean current is also to the N and NNW, and the mean current on the crest was approximately  $10^\circ$  behind that on the stoss side. The moderate waves ( $H_s = 2.5$  m) during this storm did not cause suppression of the total mean current.

## 2.4 Bedforms

Bedform wavelength and crest direction were estimated from the seafloor images. Small bedforms (Figure 6a) were present for most of the experiment. The appearance of medium wavelength bedforms occurs during storm spin-up on yearday 22 and at the peak of the storm on yearday 31. These bedforms were irregular with many terminations, as shown in Figure 6b. Large irregular bedforms were observed briefly near the peak of the first storm and displayed crescentic-shaped crests (Figure 6c).

Figure 7 shows that small bedforms had a variety of orientations. There does not appear to be a direct relationship with current direction, Figure 7c.

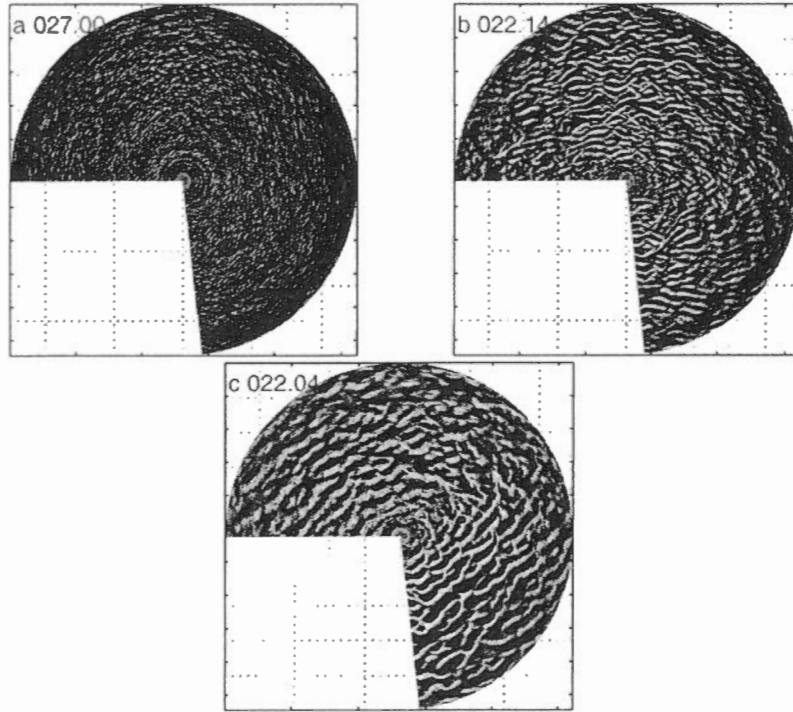


Figure 6: Fan-beam images of small, medium and large wavelength bedstates. Time in day.hour is given in the upper left corner, and each image has a radius of approximately 20 m. Positive  $Y$  is toward the top of the page.

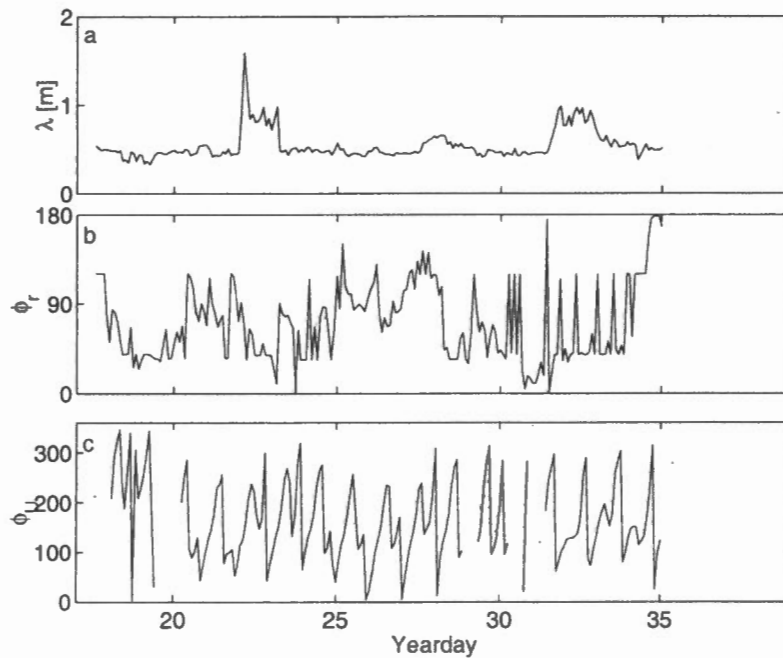


Figure 7: Time series of the bedform wavelength,  $\lambda$ , bedform orientation,  $\phi_r$ , the current direction,  $\phi_U$ .

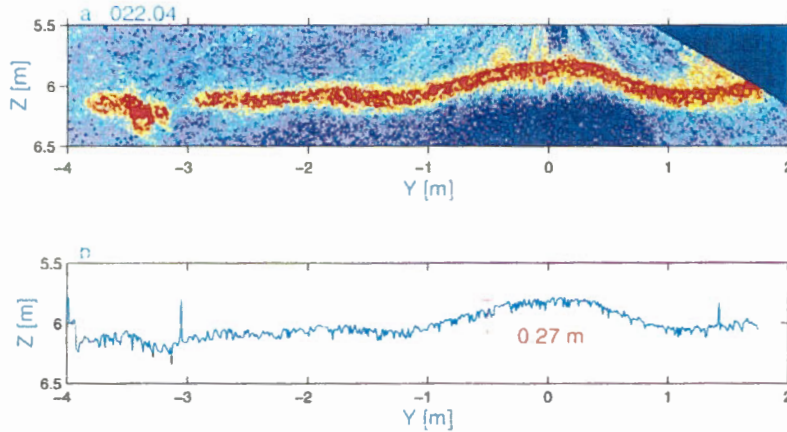


Figure 8: a) Y-Z Pencil-beam image of the bedstate on yearday 22 at 4 am. b) Extracted seafloor profile from the pencil-beam image.

## 2.5 Mobile Layer Depth

One of the objectives this analysis was to determine the maximum depth of the mobile layer for the experiment and compare the present observations to predictions by *Li et al.* [1999]. The maximum depth of the mobile layer is estimated from the greater of the bedform amplitude or the seafloor elevation change.

Bedform height for the large wavelength bedforms near the peak of the storm on yearday 22 was estimated to be 27 cm (Figure 8). The seafloor profile was taken as the location of the maximum in the pencil-beam backscatter amplitude. A mobile layer depth based on half the bedform height would be 13.5 cm.

Seafloor elevation changes were also estimated from the vertically oriented ABS's and the pencil-beam bottom location when the transducer was oriented vertically downwards. The bottom was identified as the position of the maximum backscatter amplitude. A time series of the bed elevation, Figure 9 indicates that a change in bed elevation of approximately 30 cm occurred for 3 ABS sensors and the pencil beam from midnight to 4 am on yearday 22. After the storm, the bed slowly eroded until a second modest accretion event occurred during the storm on yearday 31.

An alternative hypothesis for the seafloor elevation changes is that the quad frame settled into the sediment during the storm, and that accumulation did not occur. Settling of the instrument frame would result in a change in average depth, but the pressure sensor resolution limits and tidal fluctuations preclude an accurate estimate of the settling depth. Instead, settling estimates were estimated from by comparing pressure data from Ralph and the S4. The S4 depth time series was first corrected for settling. This was accomplished by removing the tidal energy and observing any elevation changes due to the instrument frame settling. These elevation changes were removed and the tidal components were added back in. Information on the tidal analysis is given in Appendix A. Then, the depth time series from Ralph was subtracted from the corrected depth time series from the S4, Figure 10b. The magnitude of the difference based on 2nd order fitted polynomials is 17 cm, approximately half of the estimated 30 cm change in bed elevation. However, there is clearly residual tidal energy present, and thus the estimated sinking depth is uncertain.

The estimated mobile depth based on the maximum change in elevation during the storm is within the range of 13 to 30 cm. A least-squares fit by *Li et al.* [1999] of the data collected during previous deployments in 1996 and 1997 predicted the mobile depth,  $d_m$  as

$$d_m = 0.061H_s \quad (1)$$

where  $H_s$  is the significant wave height. This empirical result predicts a mobile depth layer of 17.5 cm for

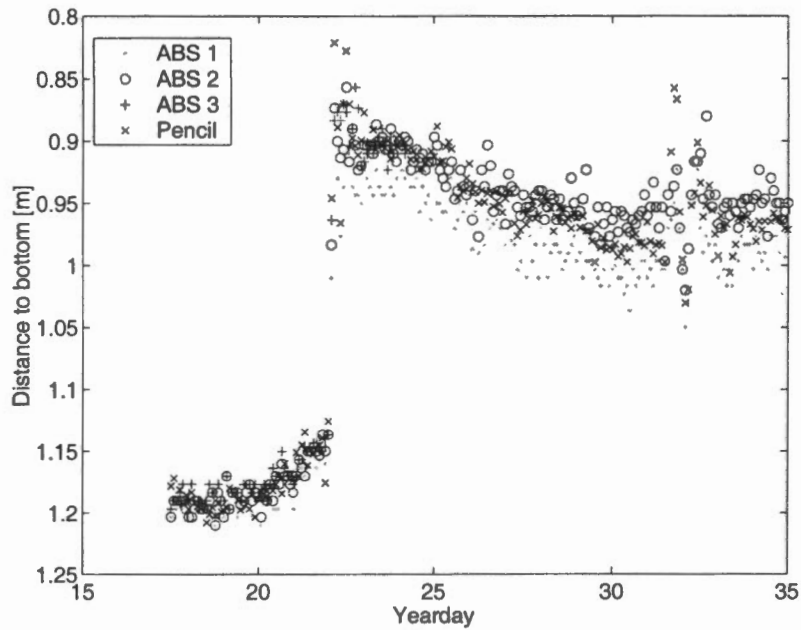


Figure 9: Time series of the seafloor elevation during the experiment. Distance to bottom was estimated from the 3 ABS's as well as from the pencil beam when the transducer was oriented vertically.

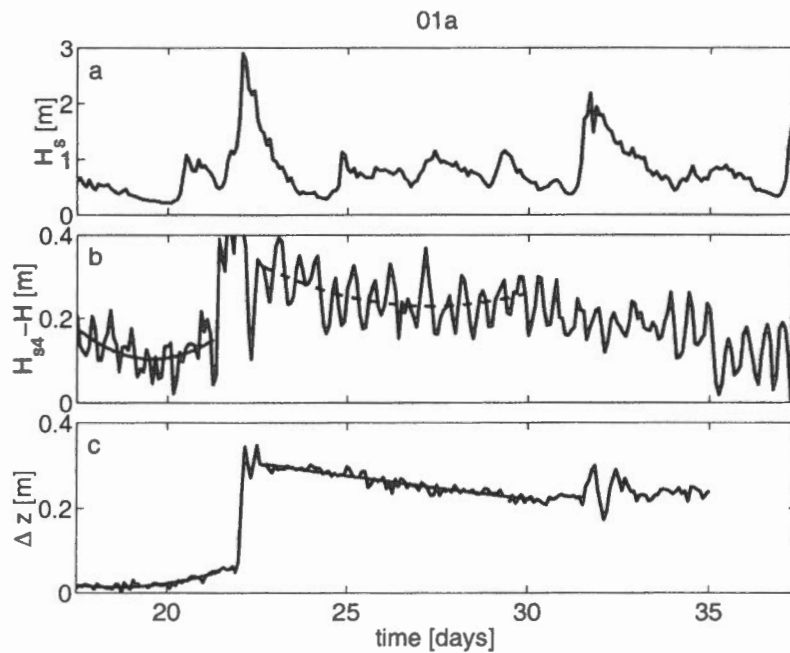


Figure 10: Time series of: (a) the significant wave height, (b) the depth time series from Ralph subtracted from the S4 data, and (c) the estimated change in bed elevation from the ABS and pencil data.

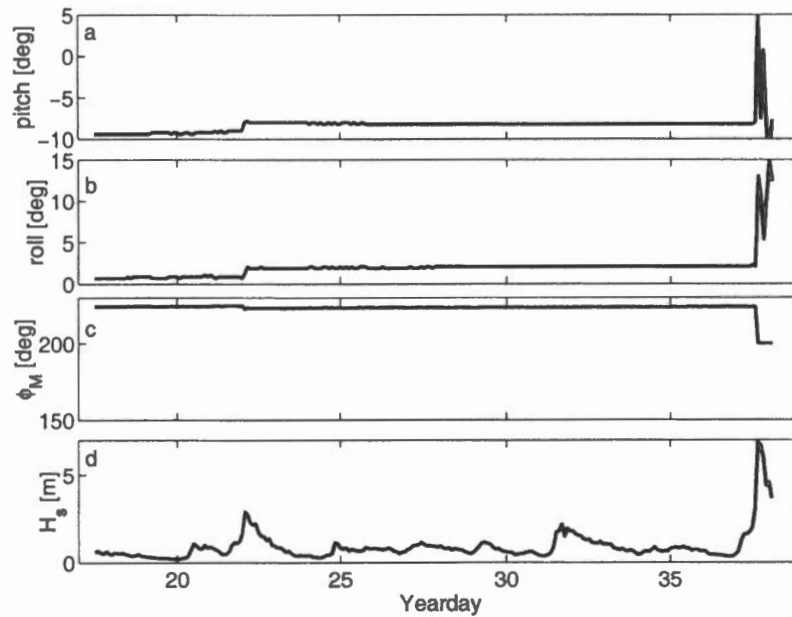


Figure 11: Time series of: (a) pitch, (b) roll, (c) compass heading,  $\phi_M$ , of the instrument frame and (d) significant wave height. Note these time series extend past yearday 35.

a significant wave height of 2.85 m. The present observation is consistent with this result.

Estimates of the pitch and roll of the instrument frame were measured by a tilt sensor which was located in the main pressure case. A change of approximately  $1^\circ$  occurred in both the pitch and roll time series during the first storm on yearday 22 (Figure 11). This modest change does not account for the large change in seafloor elevation measured by 3 ABS's and the pencil-beam. A significant change in the pitch, roll, and compass heading occurred during a storm on yearday 38. During this storm the significant wave height exceeded 8 m, and the instrument frame was moved approximately 750 m away from its original location. Wave velocities were not recorded for this storm as the current meters stopped working on yearday 34. The instrument frame likely flipped onto its side and tumbled as the buoy line was found wrapped around the frame when it was recovered. Pitch and roll estimates cannot be used to confirm this hypothesis as tilt estimates are unreliable when the instrument frame is tilted past  $\pm 60^\circ$ .

## 2.6 Sediment Suspension

Suspended sediment levels were made by OBS and ABS sensors. Figure 12 shows that both sensors had elevated levels during storm conditions. The OBS is more sensitive to fine particles, and shows elevated levels during relatively low energy conditions.

## 3 Predictions by SEDTRANS96

SEDTRANS96 is a combined wave-current bottom boundary layer model that predicts bed shear stresses, suspended sediment transport rates, bedload sediment transport rates and bedload transport direction [Li and Amos, 2001]. Measurements of depth, current velocity, current direction, wave direction, wave period and grain diameter were input into the model (Appendix B). Additional input parameters were a sediment density of  $2.65 \text{ g/cm}^3$ , fluid density of  $1.025 \text{ g/cm}^3$ , bed slope of zero, and initial flat bed. Predicted sediment transport rates from SEDTRANS96 are shown in Table B-1 and predicted bottom boundary layer

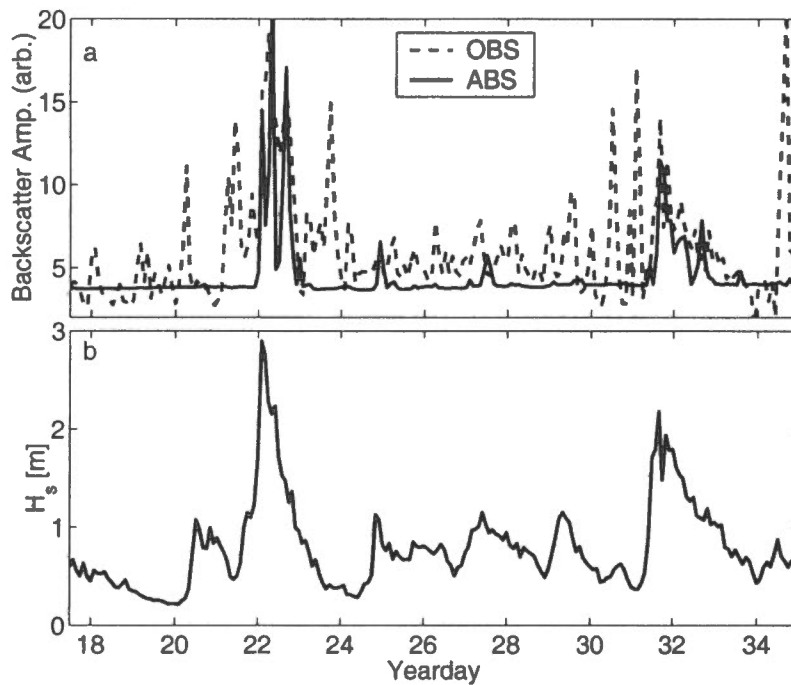


Figure 12: Time series of: (a) backscatter amplitude from the OBS4 and ABS1 at the same height above seabed and (b) significant wave height. The height of the OBS and ABS sample volume was approximately 40 cm before yearday 22, and approximately 20 cm for the latter part of the experiment.

parameters are in Table B-2. Maximum predicted sediment transport rates were 0.02 kg/m/s for bedload at a direction of 345 degrees and 0.36 kg/m/s for suspended load on yeardays 23 and 22 respectively. For the larger storm recorded by the S4, the maximum values were 0.18 kg/m/s for bedload and 8.26 kg/m/s and suspended load on yearday 37 (Tables B-3 and B-4). These values are generally higher than previous predictions due to the unusually high wave energy in addition to attenuation corrections for depth.

## 4 Acknowledgments

The authors would like to thank Edward King for creating the Sable Island Bank multi-beam bathymetry image, Figure 1. Bob Murphy, Fred Jodrey Ken Aspery, Tony Atkinson and Donny Clattenburg provided field, technical and laboratory assistance.

## References

- Heffler, D. E., A dynamic instruments for sediment dynamics, in *Proc. of Oceans '96, IEEE*, pp. 728–732, 1996.
- Li, M. Z., and C. L. Amos, SEDTRANS96; the upgraded and better calibrated sediment-transport model for continental shelves, *Computers and Geosciences*, 27, 619–645, 2001.
- Li, M. Z., C. L. Amos, and D. E. Heffler, Hydrodynamics and seabed stability observations on Sable Island Bank: A summary of the data for 1996/1997, *Tech. Rep. 2997*, Geological Survey of Canada - Atlantic, 1999.

Pawlowicz, R., B. Beardsley, and S. Lentz, Classical tidal harmonic analysis including error estimates in matlab using T\_tide, *Computers and Geosciences*, 2002.

## A Tidal Analysis

A tidal package developed by Mike Forman called T\_tide, was used to estimate the harmonic analysis of oceanic tides. The original Fortran code was re-written in Matlab by Steve Lentz, Bob Beardsley and Rich Pawlowicz, and is available on-line *Pawlowicz et al.* [2002].

Table A-1 lists the frequencies, amplitudes and phases of the harmonic constants for the S4 pressure data. The ratio of the variance predicted to the original variance is 86.9%. The relative importance of the diurnal tide to the semi-diurnal tide based on the ratio

$$\frac{H_{O1} + H_{K1}}{H_{M2}} \quad (2)$$

is small (0.24), indicating the tide is regular semi-diurnal.

Table A-1: Harmonic constants of the tidal constituents for the S4 depth time series

Constituent	Frequency [cph]	Amplitude [m]	Amplitude Error [m]	Phase Lag Greenwich [deg]
*MM	0.0015122	0.0160	0.016	329.82
MSF	0.0028219	0.0810	0.015	34.45
ALP1	0.0343966	0.0032	0.012	112.06
2Q1	0.0357064	0.0064	0.012	359.87
Q1	0.0372185	0.0161	0.016	53.12
O1	0.0387307	0.0502	0.016	76.85
NO1	0.0402686	0.0102	0.018	36.78
P1	0.0415526	0.0243	0.016	67.24
K1	0.0417807	0.0733	0.016	60.17
J1	0.0432929	0.0031	0.011	64.98
OO1	0.0448308	0.0028	0.015	93.88
UPS1	0.0463430	0.0081	0.013	25.25
EPS2	0.0761773	0.0090	0.013	114.51
MU2	0.0776895	0.0292	0.016	118.08
N2	0.0789992	0.1305	0.017	106.98
M2	0.0805114	0.5170	0.016	129.51
L2	0.0820236	0.0164	0.015	158.44
S2	0.0833333	0.1481	0.014	155.31
K2	0.0835615	0.0403	0.017	177.71
ETA2	0.0850736	0.0018	0.011	42.99
MO3	0.1192421	0.0037	0.012	202.32
M3	0.1207671	0.0003	0.011	106.80
MK3	0.1222921	0.0034	0.012	324.58
SK3	0.1251141	0.0039	0.011	29.19

cont'd

Constituent	Frequency [cph]	Amplitude [m]	Amplitude Error [m]	Phase Lag Greenwich [deg]
MN4	0.1595106	0.0123	0.015	152.31
M4	0.1610228	0.0238	0.016	201.45
SN4	0.1623326	0.0027	0.012	350.37
MS4	0.1638447	0.0144	0.015	310.98
S4	0.1666667	0.0059	0.012	191.81
2MK5	0.2028035	0.0007	0.011	11.71
2SK5	0.2084474	0.0022	0.011	164.18
2MN6	0.2400221	0.0010	0.010	275.45
M6	0.2415342	0.0013	0.010	289.55
2MS6	0.2443561	0.0003	0.011	190.85
2SM6	0.2471781	0.0014	0.012	275.70
3MK7	0.2833149	0.0003	0.010	2.49
M8	0.3220456	0.0007	0.011	33.35
M10	0.4025570	0.0019	0.011	72.28

## B SEDTRANS96 inputs and predictions

Table B-1 lists average wave and current parameters for each burst. These parameters were input into a sediment transport model SEDTRANS96. Predictions of sediment transport rates and boundary layer parameters are given in Tables B-1 and B-2. Similar input values and model predictions for the S4 data are given in Tables B-3 and B-4. The following list describes the column headings.

- $\delta_{cw}$  thickness of the wave-current boundary layer [cm]
- $\eta$  bedform height [cm]
- $\eta_p$  predicted ripple height [cm]
- $\lambda$  bedform wavelength [cm]
- $\lambda_p$  predicted ripple wavelength [cm]
- $\phi_{\bar{u}}$  wave direction [deg]
- $\phi_U$  current direction [deg]
- $A_{ABS}$ , suspended sediment levels from the ABS<sub>1</sub> [arb]
- $A_{OBS}$  suspended sediment levels from OBS<sub>4</sub> [arb]
- $A_b$  near-bed wave orbital amplitude [m]
- $H_s$  significant wave height [m]
- $Q_b$  Einstein-Brown estimate of mean sediment transport rate [ $\text{g m}^{-1} \text{s}^{-1}$ ]
- $Q_{b,dir}$  direction of mean sediment transport rate [deg]
- $Q_s$  mean suspended load sediment transport rate [ $\text{g m}^{-1} \text{s}^{-1}$ ]
- $T_w$  energy weighted wave period [s]
- $U$  mean current speed [cm/s]
- $f_{cw}$  combined wave-current friction factor
- $u_{*cs}$  skin friction current shear vel [cm/s]
- $u_{*c}$  total current shear vel [cm/s]
- $u_{*cw}$  total combined wave-current shear vel [cm/s]
- $u_{*cwb}$  bedload-enhanced comb. wave-current shear vel [cm/s]

$u_{*cwe}$  ripple-enhanced comb. wave-current shear vel [cm/s]  
 $u_{*cws}$  skin friction combined wave-current shear vel [cm/s]  
 $u_{*w}$  total wave shear vel [cm/s]  
 $u_{*ws}$  skin friction wave shear vel [cm/s]  
 $u_b$  near-bed maximum wave orbital velocity [m/s]  
 $z_0$  inner layer bottom roughness [cm]  
 $z_{0c}$  apparent bottom roughness above the wave boundary layer [cm]

Table B-1: Average wave and current parameters from Ralph, and SEDTRANS96 predicted outputs of ripple dimensions and sediment transport rates

Burst	Day	Depth	$H_s$	$A_{OBS}$	$U$	$\phi_U$	$T_w$	$\phi_w$	$\eta$	$\lambda$	$A_{ABS}$	$\eta_b$	$\lambda_b$	$Q_b$	$Q_s$	$Q_{lim}$
		[m]	[m]	[arb]	[cm/s]	[deg]	[s]	[deg]	[cm]	[cm]	[arb]	[cm]	[cm]	[g s <sup>-1</sup> m <sup>-1</sup> ]	[g s <sup>-1</sup> m <sup>-1</sup> ]	[deg]
1	17.50	24.56	0.60	3.90	35.2	75	8.4	101		3.73		1.5	21.7	0.33	1.59	75
2	17.58	24.75	0.67	4.16	15.5	133	8.8	113	6.0	21.1	3.77	1.9	21.7	0.01	0.84	133
3	17.67	24.57	0.56	4.00	13.8	214	8.9	117		3.73		2.9	19.5	0.00	0.00	214
8	18.08	24.84	0.56	6.22	14.4	109	8.5	120	5.6	22.0	3.73	2.9	21.7	0.01	0.00	109
9	18.17	24.79	0.53	4.26	13.7	197	8.9	107	6.2	21.8	3.74	3.1	20.7	0.00	0.00	197
10	18.25	24.53	0.52	3.46	17.6	219	8.1	105	5.7	22.1	3.74	0.0	0.0	0.00	0.00	219
11	18.33	24.18	0.55	3.15	9.9	240	7.9	108	5.1	22.0	3.74	2.5	21.7	0.00	0.00	240
12	18.42	24.10	0.47	3.03	4.5	25	7.5	100	5.6	21.4	3.74	0.0	0.0	0.00	0.00	25
13	18.50	24.35	0.44	2.74	17.3	70	7.7	140	5.9	21.6	3.74	2.5	16.7	0.01	0.00	70
14	18.58	24.70	0.39	3.33	13.3	117	7.6	138	5.1	21.3	3.73	0.0	0.0	0.00	0.00	117
15	18.67	24.69	0.38	4.00	9.0	194	8.2	123	5.5	21.7	3.75	0.0	0.0	0.00	0.00	194
16	18.75	24.51	0.42	2.99	10.3	218	8.5	120	5.0	22.2	3.74	2.2	14.9	0.00	0.00	218
17	18.83	24.13	0.46	2.89	2.5	153	8.2	128	5.1	21.6	3.75	0.0	0.0	0.00	0.00	153
18	18.92	24.00	0.37	2.65	18.7	63	8.3	131	5.8	22.0	3.74	1.8	12.3	0.01	0.00	63
19	19.00	24.26	0.35	2.98	41.6	82	7.9	108	5.0	21.2	3.74	2.5	21.7	0.50	0.00	82
20	19.08	24.68	0.34	4.97	44.2	109	8.5	139	4.8	21.9	3.76	2.2	21.7	0.72	4.12	109
21	19.17	24.89	0.31	6.43	36.6	150	8.4	124	4.8	21.9	3.78	2.3	18.9	0.23	0.00	150
22	19.25	24.68	0.29	4.15	38.3	197	9.5	43	6.2	21.2	3.77	2.3	18.9	0.28	0.00	197
23	19.33	23.01	0.27	6.00								1.9	16.1	0.13	0.00	221
24	19.42	24.05	0.27	3.14	28.4	244	9.2	73	4.2	23.7	3.77	1.8	14.8	0.06	0.00	244
34	20.25	24.79	0.27	11.13	27.0	55	8.1	6	4.7	22.3	3.82	1.5	12.6	0.04	0.00	55
35	20.33	24.44	0.37	4.57	28.6	107	9.5	345	5.2	21.4	3.83	1.8	14.8	0.06	0.00	107
36	20.42	24.04	0.71	3.66	18.7	141	9.6	352	5.7	21.6	3.83	0.0	0.0	0.04	0.02	141
37	20.50	23.98	1.08	4.20	2.7	322	10.2	359	7.2	23.4	3.83	0.0	0.0	0.00	0.00	322
38	20.58	24.25	0.97	3.72	13.1	302	10.0	356	6.6	22.1	3.84	0.0	0.0	0.01	0.03	302
39	20.67	24.66	0.79	3.83	12.0	317	9.7	5	9.0	22.6	3.99	0.4	21.7	0.00	0.16	317
40	20.75	24.77	0.78	3.64	3.2	344	10.0	1	9.2	21.3	3.85	0.8	21.7	0.00	0.02	344
41	20.83	24.42	1.00	3.16	10.5	257	9.7	9	7.1	21.2	3.85	0.9	21.7	0.00	0.17	257
42	20.92	24.19	0.84	2.72	24.1	284	9.1	10	6.4	20.5	3.82	1.9	21.7	0.06	1.81	284
43	21.00	24.02	0.89	3.04	42.2	315	9.3	16	6.6	19.9	3.85	0.0	0.0	1.10	0.14	315
44	21.08	24.81	0.81	3.10	68.3	342	9.4	12	5.9	20.7	3.83	0.0	0.0	11.92	2.63	342
45	21.17	24.84	0.75	7.44	62.8	359	9.8	10	7.8	22.9	3.88	0.0	0.0	8.16	1.72	359
46	21.25	24.96	0.66	10.46	35.4	31	9.9	14	7.0	23.1	3.82	1.2	21.7	0.39	1.24	31
47	21.33	24.62	0.50	7.62	18.4	84	9.9	4	5.8	22.4	3.77	2.2	14.6	0.01	0.00	84
48	21.42	24.29	0.47	13.92	24.6	90	9.0	109	6.4	22.3	3.80	2.8	18.4	0.04	0.00	90
49	21.50	24.02	0.51	11.81	3.1	112	8.4	331	5.5	23.7	3.84	1.0	21.7	0.00	0.02	112
50	21.58	24.14	0.63	5.89	20.9	292	7.4	105	5.5	22.6	3.86	0.0	0.0	0.05	0.02	292
51	21.67	24.01	0.61	5.70	37.2	312	8.0	293	6.4	22.9	3.85	0.0	0.0	1.26	1.27	312
52	21.75	24.89	1.15	6.51	15.2	315	8.5	308	5.7	23.3	3.83	0.0	0.0	0.03	0.13	315
53	21.83	24.55	1.10	9.41	8.7	321	8.6	354	7.2	21.2	3.81	0.0	0.0	0.00	0.02	321
54	21.92	24.15	1.23	7.49	28.0	266	8.2	160	6.6	22.5	3.84	0.0	0.0	0.45	1.22	266
55	22.00	23.95	1.70	6.03	37.3	287	10.0	6	6.8	21.4	4.76	0.0	0.0	2.34	9.01	287
56	22.08	24.04	2.90	15.65	39.4	326	12.7	16	8.1	37.2	14.51	0.0	0.0	13.02	354.85	326
57	22.17	24.48	2.76	16.24	42.5	339	13.5	30	20.0	83.2	7.58	0.0	0.0	12.47	157.08	339

cont'd

Burst	Day	Depth	$H_s$	$A_{OBS}$	$U$	$\phi_U$	$T_w$	$\phi_w$	$\eta$	$\lambda$	$A_{ABS}$	$\eta_b$	$\lambda_b$	$Q_b$	$Q_s$	$Q_{lim}$
		[m]	[m]	[arb]	[cm/s]	[deg]	[s]	[deg]	[cm]	[cm]	[arb]	[cm]	[cm]	[g s <sup>-1</sup> m <sup>-1</sup> ]	[g s <sup>-1</sup> m <sup>-1</sup> ]	[deg]
58	22.25	24.87	2.28	19.20	22.1	9	12.7	28	5.2	40.6	10.98	0.0	0.0	0.78	22.37	9
59	22.33	24.71	2.16	14.63	15.5	61	12.6	31	10.2	40.8	21.38	0.0	0.0	0.14	5.05	61
60	22.42	24.26	2.24	13.79	19.4	91	11.9	43	6.9	34.5	4.90	0.0	0.0	0.39	10.79	91
61	22.50	23.90	1.72	11.88	12.0	75	10.8	44	3.5	31.5	5.40	0.0	0.0	0.03	0.65	75
62	22.58	23.88	1.53	13.26	8.2	28	11.2	52	4.1	29.3	10.67	0.0	0.0	0.00	0.24	28
63	22.67	24.29	1.47	15.93	12.7	360	11.1	46	3.9	31.8	17.08	0.0	0.0	0.03	0.40	360
64	22.75	24.67	1.25	13.45	9.7	19	10.6	44	3.6	32.1	8.58	0.0	0.0	0.01	0.09	19
65	22.83	24.60	1.37	10.05	11.3	152	11.3	46	7.2	33.9	5.77	0.0	0.0	0.01	0.14	152
66	22.92	24.30	0.99	6.98	5.7	255	10.7	28	5.8	33.7	4.01	0.0	0.0	0.00	0.00	255
67	23.00	24.00	0.97	3.66	20.1	286	10.7	46	4.3	33.0	5.58	0.4	21.7	0.06	0.43	286
68	23.08	24.05	0.84	3.36	41.7	322	10.1	48			3.88	0.2	21.7	0.97	1.20	322
69	23.17	24.45	0.87	8.26	72.9	345	10.0	28	4.5	33.9	3.95	0.0	0.0	21.82	7.70	345
70	23.25	24.95	0.75	8.11	57.9	4	9.8	40	6.0	24.2	3.98	0.0	0.0	6.28	1.17	4
71	23.33	24.94	0.60	5.72	33.6	41	10.0	50	6.8	24.0	3.74	1.5	21.7	0.35	1.67	41
72	23.42	24.48	0.67	6.89	25.6	97	9.6	46	5.1	24.4	3.68	2.2	21.7	0.10	2.84	97
73	23.50	24.01	0.53	7.73	19.3	121	9.9	38	5.5	24.0	3.70	2.7	17.9	0.02	0.00	121
74	23.58	23.88	0.43	6.20	3.5	94	9.3	28	6.2	24.1	3.71	0.0	0.0	0.00	0.00	94
75	23.67	24.20	0.37	10.54	15.9	345	9.6	19	5.2	24.6	3.72	2.3	15.2	0.01	0.00	345
76	23.75	24.73	0.42	14.94	10.4	23	9.4	26	5.0	24.4	3.73	0.0	0.0	0.00	0.00	23
77	23.83	24.81	0.38	8.36	12.1	132	9.7	32	5.1	25.0	3.73	0.0	0.0	0.00	0.00	132
78	23.92	24.50	0.38	5.77	6.4	173	9.1	46	5.4	25.6	3.77	0.0	0.0	0.00	0.00	173
79	24.00	24.11	0.39	4.39	16.5	278	9.1	22	4.6	25.3	3.81	0.0	0.0	0.00	0.00	278
80	24.08	23.98	0.41	3.71	46.9	315	9.1	356	5.0	24.4	3.86	2.0	21.7	1.11	4.19	315
81	24.17	24.33	0.32	7.65	74.9	343	8.9	344	5.1	24.3	3.87	0.0	0.0	12.33	0.53	343
82	24.25	24.82	0.31	6.82	73.3	1	10.1	8	5.4	24.6	3.78	0.0	0.0	12.27	0.68	1
83	24.33	25.06	0.30	4.10	47.7	27	9.7	16	5.2	24.4	3.70	2.5	21.7	1.04	0.00	27
84	24.42	24.71	0.28	4.65	29.4	84	7.6	330	5.9	24.4	3.67	0.0	0.0	0.00	0.00	84
85	24.50	24.14	0.34	4.80	26.9	117	7.8	344	5.3	24.8	3.67	2.7	17.7	0.06	0.00	117
86	24.58	23.91	0.42	4.76	4.3	129	7.7	357	5.8	24.4	3.67	2.5	17.0	0.00	0.00	129
87	24.67	24.11	0.43	5.00	11.0	310	7.8	2	5.8	24.1	3.68	2.8	18.4	0.00	0.00	310
88	24.75	24.61	0.51	4.86	19.6	322	8.3	347	5.4	24.8	3.69	2.1	21.7	0.03	1.61	322
89	24.83	24.85	1.13	5.33	5.2	356	9.7	343	5.7	25.6	4.00	0.0	0.0	0.00	0.01	356
90	24.92	24.61	1.08	6.12	2.4	287	9.7	347	6.5	22.6	4					

Table B-2: Boundary layer parameters output from SEDTRANS96 for Ralph input

Burst Day	Depth $H_b$	$A_{OBS}$	$U$	$\phi_U$	$T_w$	$\phi_s$	$\eta$	$\lambda$	$A_{LBS}$	$\eta_b$	$\lambda_b$	$Q_b$	$Q_s$	$Q_{b,dir}$
[m]	[m]	[m]	[cm/s]	[deg]	[cm]	[deg]	[cm]	[m]	[cm]	[cm]	[cm]	[g s <sup>-1</sup> m <sup>-1</sup> ]	[g s <sup>-1</sup> m <sup>-1</sup> ]	[deg]
17.50	0.22	0.29	1.24	1.8	2.2	2.8	3.6	5.0	3.1	4.9	5.8	6.1	0.2	1.0
17.58	0.28	0.39	1.25	1.0	2.4	2.6	3.6	4.7	1.8	5.7	6.0	6.8	0.2	2.6
17.67	0.23	0.33	1.37	0.9	2.0	2.0	3.8	3.2	1.6	5.8	5.9	6.7	0.4	3.1
18.08	0.24	0.32	1.32	0.9	2.1	2.3	4.0	4.0	1.7	6.0	6.3	6.8	0.4	3.2
18.17	0.25	0.35	1.35	0.9	2.1	2.1	3.9	3.5	1.7	6.2	6.3	7.1	0.5	3.4
18.25	0.12	0.16	1.62	0.9	1.3	1.4	1.4	0.9	1.3	1.4	1.5	0.0	0.0	0.0
18.33	0.27	0.34	1.35	0.7	2.3	2.4	3.7	4.3	1.2	6.2	6.3	6.3	0.3	3.6
18.42	0.17	0.20	1.63	0.3	1.5	1.5	1.5	0.3	1.5	1.5	1.5	0.0	0.4	0.4
18.50	0.18	0.22	1.51	1.0	1.7	1.8	3.4	2.6	1.8	4.9	5.0	4.9	0.4	1.9
18.58	0.13	0.16	1.62	0.8	1.4	1.6	1.6	1.6	0.8	1.4	1.6	1.5	0.0	0.1
18.67	0.13	0.17	1.68	0.5	1.3	1.3	1.3	0.5	1.3	1.3	1.4	0.0	0.1	0.1
18.75	0.19	0.26	1.49	0.7	1.7	1.7	3.2	2.3	1.2	4.7	4.7	5.1	0.3	2.6
18.83	0.17	0.23	1.56	0.2	1.6	1.6	1.6	1.6	0.2	1.6	1.6	1.6	0.0	0.7
18.92	0.15	0.19	1.54	1.0	1.4	1.6	3.0	1.7	1.7	3.7	3.9	4.1	0.3	1.2
19.00	0.15	0.18	1.31	1.9	1.7	2.6	4.1	4.3	3.7	4.5	5.8	5.8	0.4	1.0
19.08	0.16	0.21	1.25	2.1	1.8	2.7	3.9	4.5	3.8	4.4	5.7	6.2	0.3	0.8
19.17	0.13	0.17	1.34	1.7	1.5	2.3	3.6	3.5	3.1	3.8	4.9	5.2	0.3	0.9
19.25	0.12	0.18	1.27	1.8	1.5	2.3	3.6	3.5	3.3	3.6	4.8	5.9	0.3	0.8
19.33	0.10	0.16	1.34	1.6	1.3	2.0	3.2	2.9	2.8	3.1	4.1	4.9	0.3	0.7
19.42	0.11	0.16	1.38	1.4	1.3	1.9	3.0	2.7	2.4	3.1	3.9	4.6	0.2	0.7
20.25	0.11	0.14	1.52	1.3	1.3	1.7	2.8	2.2	2.1	2.9	3.5	3.6	0.2	0.6
20.33	0.14	0.21	1.37	1.4	1.5	1.9	3.0	2.7	2.4	3.5	4.0	4.8	0.2	0.8
20.42	0.37	0.56	1.12	1.3	3.0	3.2	3.2	6.3	2.0	6.0	6.3	7.7	0.1	2.2
20.50	0.49	0.79	1.06	0.3	3.5	3.6	3.6	7.6	0.4	7.6	7.6	9.8	0.2	7.8
20.58	0.45	0.71	1.08	1.0	3.4	3.5	3.5	7.2	1.7	7.1	7.2	9.2	0.2	3.7
20.67	0.37	0.57	1.15	0.9	2.9	3.0	3.2	5.8	1.4	5.8	5.9	7.3	0.1	2.8
20.75	0.37	0.59	1.15	0.3	2.8	2.8	3.2	5.5	0.5	5.8	5.8	7.4	0.1	5.4
20.83	0.35	0.55	1.17	0.8	2.8	2.8	3.2	5.4	1.3	5.8	5.8	7.2	0.1	3.1
20.92	0.30	0.44	1.24	1.4	2.5	2.5	3.5	4.7	2.5	6.0	6.0	7.0	0.2	1.8
21.00	0.34	0.51	1.10	2.2	3.0	3.5	3.5	6.8	3.7	6.2	6.8	8.1	0.2	1.0
21.08	0.30	0.45	1.01	3.3	3.0	4.4	4.4	8.8	5.9	6.7	8.8	10.6	0.3	0.9
21.17	0.29	0.45	1.01	3.1	3.0	4.3	4.3	8.4	5.5	6.4	8.4	10.6	0.2	0.9
21.25	0.23	0.37	1.15	1.9	2.3	2.9	3.5	5.2	3.1	4.8	5.7	7.2	0.2	1.0
21.33	0.18	0.28	1.41	1.0	1.6	1.7	3.2	2.2	1.9	4.3	4.4	5.5	0.3	1.6
21.42	0.15	0.21	1.37	1.3	1.6	2.0	3.8	3.0	2.5	4.4	5.0	5.8	0.4	1.6
21.50	0.35	0.46	1.24	0.3	2.7	2.8	3.2	5.4	0.4	5.9	5.9	6.2	0.1	4.8
21.58	0.33	0.39	1.24	1.3	2.9	3.2	3.2	6.3	2.1	6.0	6.3	6.0	0.1	1.7
21.67	0.46	0.59	1.06	2.3	3.9	4.5	4.5	9.8	4.1	8.9	9.8	10.0	0.3	2.2

cont'd

Day	$u_b$	$A_b$	$f_{cws}$	$u_{cs}$	$u_{ws}$	$u_{cws}$	$u_{cws}$	$u_{cws}$	$u_{cs}$	$u_{ws}$	$u_{cws}$	$\delta_{cws}$	$z_0$	$z_{0c}$
[m]	[m]	(x 100)	[cm/s]	[cm/s]	[cm/s]	[cm/s]	[cm/s]	[cm/s]	[cm/s]	[cm/s]	[cm/s]	[cm]	[cm]	[cm]
21.75	0.50	0.67	1.08	1.2	3.8	4.0	4.0	8.8	2.0	8.6	8.8	9.5	0.2	4.0
21.83	0.46	0.63	1.12	0.8	3.5	3.6	3.6	7.6	1.2	7.6	7.6	8.4	0.2	4.6
21.92	0.60	0.78	1.04	1.9	4.5	4.7	4.7	10.8	3.5	10.6	10.8	11.3	0.3	3.5
22.00	0.77	1.23	0.92	2.5	5.4	5.5	5.5	13.3	5.0	13.0	13.3	16.9	0.4	4.1
22.08	1.31	2.65	0.74	3.4	8.4	8.9	8.9	23.3	8.2	22.3	23.3	37.7	0.8	9.9
22.17	1.05	2.26	0.76	3.3	7.0	7.5	7.5	18.7	7.8	17.6	18.7	32.3	0.6	6.3
22.25	0.96	1.95	0.80	2.1	6.4	6.7	6.7	16.5	4.6	15.9	16.5	26.7	0.5	8.9
22.33	0.88	1.76	0.83	1.6	5.8	6.0	6.0	14.4	3.2	14.1	14.4	23.1	0.4	9.5
22.42	0.92	1.73	0.84	1.9	6.1	6.3	6.3	15.4	4.0	15.0	15.4	23.3	0.5	8.5
22.50	0.68	1.16	0.93	1.2	4.8	4.9	4.9	11.3	2.3	11.1	11.3	15.5	0.3	7.0
22.58	0.66	1.17	0.94	0.9	4.6	4.7	4.7	10.6	1.7	10.5	10.6	15.1	0.3	8.2
22.67	0.63	1.12	0.95	1.2	4.5	4.6	4.6	10.3	2.2	10.1	10.3	14.5	0.3	6.2
22.75	0.54	0.90	1.01	0.9	3.9	4.0	4.0	8.7	1.6	8.6	8.7	11.7	0.2	5.6
22.83	0.58	1.04	0.97	1.1	4.1	4.1	4.1	9.0	1.9	8.9	9.0	13.0	0.2	5.6
22.92	0.42	0.71	1.08	0.6	3.1	3.2	3.2	6.4	0.9	6.3	6.4	8.7	0.1	4.9
23.00	0.36	0.61	1.10	1.4	2.8	3.0	3.2	5.8	2.2	5.7	5.9	8.0	0.1	1.7
23.08	0.34	0.56	1.11	2.2	2.8	3.1	3.2	6.0	3.7	5.7	6.0	7.7	0.1	0.7
23.17	0.34	0.54	0.97	3.6	3.4	4.8	4.8	9.9	7.0	7.6	9.9	12.6	0.3	0.9
23.25	0.30	0.46	1.03	3.0	2.9	4.1	4.1	8.1	5.4	6.3	8.1	10.1	0.2	0.8
23.33	0.22	0.35	1.16	1.8	2.2	2.8	3.6	5.1	3.2	4.7	5.7	7.3	0.2	1.0
23.42	0.25	0.38	1.22	1.5	2.2	2.5	3.8	4.5	2.8	5.5	6.0	7.3	0.3	1.6
23.50	0.21	0.33	1.34	1.1	1.8	1.9	3.6	2.9	2.2	5.1	5.2	6.6	0.4	2.0
23.58	0.15	0.22	1.57	0.3	1.4	1.4	1.4	1.4	0.3	1.4	1.4	1.6	0.0	0.4
23.67	0.15	0.23	1.41	0.9	1.5	1.7	3.3	2.3	1.8	4.0	4.3	5.3	0.3	1.7
23.75	0.14	0.22	1.49	0.7	1.4	1.5	1.5	1.5	0.7	1.4	1.5	1.8	0.0	0.1
23.83	0.14	0.21	1.56	0.7	1.3	1.3	1.3	1.3	0.7	1.3	1.3	1.7	0.0	0.1
23.92	0.13	0.19	1.63	0.4	1.2	1.3	1.3	1.3	0.4	1.2	1.3	1.5	0.0	0.2
24.00	0.13	0.19	1.56	0.9	1.3	1.4	1.4	1.4	0.9	1.3	1.4	1.6	0.0	0.0
24.08	0.15	0.22	1.20	2.2	1.8	2.8	3.9	4.7	4.1	4.2	5.7	6.6	0.3	0.7
24.17	0.10	0.14	1.10	3.3	1.7	3.7	3.7	6.7	5.7	5.7	6.7	7.5	0.2	0.3
24.25	0.13	0.20	1.04	3.3	1.9	3.8	3.8	6.9	5.8	5.8	6.9	8.9	0.2	0.4
24.33	0.10	0.16	1.20	2.2	1.5	2.6	4.1	4.3	4.3	3.6	5.6	7.0	0.4	0.7
24.42	0.07	0.08	1.64	1.3	1.0	1.5	1.5	1.5	1.3	1.0	1.5	1.5	0.0	0.0
24.50	0.13	0.17	1.47	1.4	1.5	1.9	3.6	2.9	2.7	4.2	4.9	4.8	0.4	1.2
24.58	0.20	0.25	1.51	0.4	1.8	1.8	3.4	2.7	0.6	5.2	5.3	5.2	0.4	3.8
24.67	0.20	0.25	1.47	0.7	1.8	1.9	3.6	3.0	1.4	5.4	5.5	5.5	0.4	2.9
24.75	0.25	0.33	1.28	1.2	2.3	2.6	3.7	4.6	2.2	5.6	6.0	6.4	0.3	2.0
24.83	0.48	0.74	1.08	0.5	3.5	3.6	3.6	7.6	0.9	7.6	7.6	9.4	0.2	6.0
24.92	0.45	0.69	1.10	0.3	3.3	3.3	3.3	7.0	0.4	7.0	7.0	8.6	0.2	6.8
25.00	0.36	0.49	1.18	1.7	2.9	3.1	3.1	6.2	2.8	5.9	6.2	6.8	0.1	1.2
25.08	0.35	0.53	1.08	2.3	3.1	3.7	3.7	7.4	4.0	6.5	7.4	8.8	0.2	1.1
25.17	0.32	0.45	1.05	2.9	3.1	4.2	4.2	8.6	5.3	6.9	8.6	9.8	0.2	1.0

cont'd

Day	$u_b$	$A_b$	$f_{cws}$	$u_{cs}$	$u_{ws}$	$u_{cws}$	$u_{cws}$	$u_{cws}$	$u_{cs}$	$u_{ws}$	$u_{cws}$	$\delta_{cws}$	$z_0$	$z_{0c}$
[m]	[m]	(x 100)	[cm/s]	[cm/s]	[cm/s]	[cm/s]	[cm/s]	[cm/s]	[cm/s]	[cm/s]	[cm/s]	[cm]	[cm]	[cm]
25.25	0.25	0.36	1.05	3.2	2.8	4.2	4.2	8.3	5.8	6.1	8.3	9.5	0.2	0.8
25.33	0.29	0.45	1.08	2.5	2.8	3.5	3.5	6.9	4.3	5.7	6.9	8.4	0.2	0.8
25.42	0.24	0.37	1.29	1.4	2.1	2.2	4.1	3.6	3.0					



Burst	Day	Depth	$H_s$	$U$	$\phi_U$	$T_w$	$\phi_w$	$\eta$	$\lambda_b$	$Q_b$	$Q_s$	$Q_{b,s}$
		[m]	[m]	[cm/s]	[deg]	[s]	[deg]		[cm]	[cm]	[g s m <sup>-1</sup> ]	[g s m <sup>-1</sup> ]
156	30.30	32.82	0.72	20.17	357	9.53	27	2.9	19.1	0.03	0.00	12
157	30.39	33.33	0.92	21.45	12	8.85	22	2.4	16.2	0.02	0.00	63
158	30.47	33.61	0.97	20.80	63	8.97	270	3.7	26.0	0.02	0.00	104
159	30.55	33.36	2.17	15.89	103	8.68	290	4.0	26.6	0.01	0.00	147
160	30.64	32.87	1.93	15.67	147	8.95	284	3.3	21.8	0.00	0.00	176
161	30.72	32.60	1.93	7.11	176	8.66	279	0.0	0.0	0.00	0.00	0
162	30.80	32.74	1.13	2.26	282	9.48	84	2.3	15.6	0.00	0.00	18
163	30.89	33.19	1.39	6.86	18	9.35	83	0.0	0.0	0.00	0.00	0
164	30.97	33.57	0.35	4.49	66	9.15	82	0.0	0.0	0.00	0.00	0
165	31.05	33.43	0.27	4.96	143	10.25	59	0.0	0.0	0.00	0.00	0
166	31.14	33.04	0.26	7.09	186	9.68	28	0.0	0.0	0.00	0.00	0
167	31.22	32.75	0.66	5.52	300	9.23	50	0.0	0.0	0.00	0.00	0
168	31.30	32.73	0.88	14.32	356	8.69	42	1.7	26.0	0.05	0.64	41
169	31.39	33.07	2.91	20.04	41	8.30	92	0.0	0.0	0.15	0.05	85
170	31.47	33.39	3.70	22.91	85	8.29	88	0.0	0.0	0.12	0.22	139
171	31.55	33.29	3.55	18.80	139	10.56	62	0.0	0.0	0.07	0.13	184
172	31.64	32.91	2.90	16.39	184	11.79	49	0.0	0.0	0.02	0.09	260
173	31.72	32.65	3.17	11.94	260	10.92	47	0.0	0.0	0.22	0.26	291
174	31.80	32.61	3.22	22.001	291	10.90	44	0.0	0.0	0.26	0.13	324
175	31.89	32.99	2.83	24.24	324	11.42	40	0.0	0.0	0.27	0.07	343
176	31.97	33.49	2.58	25.80	343	10.87	41	0.0	0.0	0.01	0.02	359
177	32.05	33.57	2.73	10.36	359	11.51	46	0.0	0.0	0.01	0.02	5
178	32.14	33.24	2.71	10.83	5	11.01	59	0.0	0.0	0.00	0.01	1
179	32.22	32.86	2.54	8.78	1	11.25	45	0.6	26.0	0.02	0.17	6
180	32.30	32.70	2.14	13.67	6	11.08	36	0.2	26.0	0.01	0.13	16
181	32.39	32.93	2.29	12.03	16	10.88	42	0.6	26.0	0.00	0.10	32
182	32.47	33.34	2.20	9.73	32	11.35	45	3.8	25.4	0.00	0.00	78
183	32.55	33.41	1.60	4.54	78	11.13	42	4.0	27.0	0.00	0.00	204
184	32.64	33.15	1.59	7.31	204	11.44	42	4.2	27.8	0.00	0.00	248
185	32.72	32.82	1.80	5.84	248	10.42	43	3.2	26.0	0.01	0.00	274
186	32.80	32.61	1.73	13.10	274	10.97	42	2.8	26.0	0.04	0.00	326
187	32.89	32.77	2.10	19.56	326	10.04	58	3.0	26.0	0.09	0.00	360
188	32.97	33.24	1.71	23.67	360	10.19	46	3.9	26.2	0.01	0.00	20
189	33.05	33.47	1.68	13.64	19	9.96	56	3.9	25.7	0.00	0.00	56
190	33.14	33.28	1.74	9.44	56	9.76	58	0.0	0.0	0.00	0.00	0
191	33.22	33.00	0.94	7.54	68	9.61	52	3.0	19.7	0.00	0.00	61
192	33.30	32.71	1.40	6.25	61	9.76	72	3.4	22.7	0.00	0.00	39
193	33.39	32.70	1.50	7.60	39	10.01	53	3.3	22.2	0.00	0.00	35
194	33.47	33.07	1.51	9.67	35	9.69	57	2.4	16.1	0.00	0.00	90
195	33.55	33.36	1.12	7.86	90	10.48	69	0.0	0.0	0.00	0.00	0
196	33.64	33.23	1.01	6.79	141	9.85	55	0.0	0.0	0.00	0.00	0
197	33.72	32.99	1.06	4.94	177	10.03	60	0.0	0.0	0.00	0.00	0
198	33.80	32.70	1.08	5.57	270	9.83	60	0.0	0.0	0.00	0.00	0
199	33.89	32.62	1.13	15.18	320	8.97	37	3.0	20.1	0.05	0.00	353
200	33.97	33.06	1.00	24.81	353	9.30	26	2.5	16.7	0.02	0.00	16
201	34.05	33.52	0.95	20.29	16	9.10	24	0.0	0.0	0.00	0.00	0
202	34.14	33.53	0.62	11.47	31	8.69	282	3.6	24.3	0.00	0.00	37
203	34.22	33.31	2.18	4.40	37	8.68	86	0.0	0.0	0.00	0.00	0

cont'd

28

Burst	Day	Depth	$H_s$	$U$	$\phi_U$	$T_w$	$\phi_w$	$\eta$	$\lambda_b$	$Q_b$	$Q_s$	$Q_{b,s}$
		[m]	[m]	[cm/s]	[deg]	[s]	[deg]		[cm]	[cm]	[g s m <sup>-1</sup> ]	[g s m <sup>-1</sup> ]
204	34.30	32.90	1.80	3.89	355	7.91	79	2.8	18.6	0.00	0.00	346
205	34.39	32.70	1.81	8.31	346	8.32	287	4.1	27.2	0.01	0.00	1
206	34.47	32.87	1.97	14.75	1	8.97	327	3.2	21.7	0.00	0.00	26
207	34.55	33.29	1.91	8.36	26	8.86	302	0.0	0.0	0.00	0.00	0
208	34.64	33.41	1.54	2.87	69	8.73	327	0.0	0.0	0.00	0.00	0
209	34.72	33.21	1.35	0.33	258	9.13	325	0.0	0.0	0.00	0.00	0
210	34.80	32.87	1.20	7.13	231	9.03	271	0.0	0.0	0.00	0.00	0
211	34.89	32.63	1.18	13.05	308	9.39	63	3.3	26.0	0.15	0.00	349
212	34.97	32.81	1.45	27.35	349	9.75	347	1.6	26.0	0.35	1.04	11
213	35.05	33.30	1.62	31.58	11	10.17	17	3.0	26.0	0.11	0.00	34
214	35.14	33.63	1.51	24.68	34	10.44	37	4.1	27.1	0.03	0.00	65
215	35.22	33.51	1.46	19.55	65	10.40	44	3.4	22.7	0.01	0.00	91
216	35.30	33.12	1.35	14.15	91	10.18	61	3.0	20.2	0.00	0.00	104
217	35.39	32.72	1.35	7.35	104	10.12	75	2.9	19.3	0.00	0.00	84
218	35.47	32.67	1.44	3.61	84	9.73	68	0.0	0.0	0.00	0.00	0
219	35.55	33.00	0.96	3.77	67	9.28	80	0.0	0.0	0.00	0.00	0
220	35.64	33.43	1.06	3.96	143	9.61	72	3.0	19.7	0.00	0.00	196
221	35.72	33.37	1.40	11.15	196	9.57	63	3.6	24.2	0.01	0.00	238
222	35.80	33.04	1.46	14.61	238	9.82	59	3.7	24.6	0.03	0.00	271
223	35.89	32.64	1.38	19.93	271	9.64	66	3.4	22.8	0.03	0.00	328
224	35.97	32.62	1.42	20.69	328	9.26	21	2.8	23.5	0.26	0.00	1
225	36.05	33.03	1.13	34.31	1	9.38	40	2.4	20.1	0.16	0.00	26
226	36.14	33.56	0.87	32.15	25	9.38	41	1.7	13.8	0.02	0.00	52
227	36.22	33.68	0.79	22.11	52	9.57	44	0.0	0.0	0.00	0.00	0
228	36.30	33.35	0.72	12.15	114	9.74	76	0.0	0.0	0.00	0.00	0
229	36.39	32.79	0.78	10.61	167	9.54	26	0.0	0.0	0.00	0.00	0
230	36.47	32.52	0.66	8.49	236	9.40	6	0.0	0.0	0.00	0.00	0
231	36.55	32.72	0.77	13.34	284	9.31	87	0.0	0.0	0.00	0.00	0
232	36.64	33.22	0.83	11.68	293	9.38	68	0.0	0.0	0.00	0.00	0
233	36.72	33.52	0.47	12.39	270	9.29	75	0.0	0.0	0.00	0.00	0
234	36.80	33.32	0.44	15.66	260	9.28	72	0.0	0.0	0.00	0.00	0
235	36.89	32.79	0.26	32.13	272	8.44	83	0.0	0.0	0.00	0.00	0
236	36.97	32.50	0.27	35.85	301	7.64	285	2.3	19.2	0.38	0.00	336
237	37.05	32.70	0.60	41.09	336	7.94	329	0.0	0.0	2.65	0.10	356
238	37.14	33.32	2.65	49.71	356	7.89	323	0.0	0.0	1.67	0.29	11
239	37.22	33.89	3.97	40.45	11	8.33	313	0.0	0.0	0.21	0.16	26
240	37.30	33.71	3.87	22.89	26	9.22	320	0.0	0.0	0.01	0.02	53
241	37.39	33.09	3.00	10.28	53	10.33	337	0.0	0.0	0.00	0.05	30
242	37.47	32.55	3.63	5.88	30	10.60	336	0.0	0.0	0.10	0.70	70
243	37.55	32.56	4.15	15.97	70	10.86	331	0.0	0.0	3.16	155.29	76
244	37.64	32.98	7.96	24.96	76	10.82	75	0.0	0.0	42.90	4219.60	113
245	37.72	33.51	11.66	34.30	113	12.97	70	0.0	0.0	175.50	8259.37	143
246	37.80	33.69	13.11	49.07	143	12.47	79	0.0	0.0	66.16	827.18	162
247	37.89	33.29	8.29	54.55	163	12.43	72	0.0	0.0	17.03	183.21	186
248	37.97	32.74	6.19	42.60	186	12.42	69	0.0	0.0	0.08	12.89	219
249	38.05	32.69	6.22	10.47	219	12.20	74	0.0	0.0	0.08	5.86	339
250	38.14	33.34	5.92	11.75	339	11.52	61	0.0	0.0	0.00	0.35	38
251	38.22	34.08	4.95	4.59	38	11.37	73	0.0	0.0	0.04	0.84	148

cont'd

29

Burst	Day	Depth	$H_s$	$U$	$\phi_U$	$T_w$	$\phi_w$	$\eta$	$\lambda_b$	$Q_b$	$Q_s$	$Q_{b,s}$
		[m]	[m]	[cm/s]	[deg]	[s]	[deg]		[cm]	[cm]	[g s m <sup>-1</sup> ]	[g s m <sup>-1</sup> ]
252	38.30	34.27	4.77	12.45	148	10						

Burst	Day	Depth	$H_s$	$U$	$\phi_U$	$T_w$	$\phi_e$	$\eta$	$\lambda_b$	$Q_b$	$Q_s$	$Q_{s_{int}}$
		[m]	[m]	[cm/s]	[deg]	[s]	[deg]	[cm]	[cm]	[g s <sup>-1</sup> ]	[g s <sup>-1</sup> ]	[deg]
348	46.30	33.25	2.03	6.23	185	8.06	28	0.0	0.0	0.00	0.00	0
349	46.39	33.27	1.80	1.69	189	7.68	27	0.0	0.0	0.00	0.00	0
350	46.47	33.62	1.88	2.09	162	8.02	28	0.0	0.0	0.00	0.00	0
351	46.55	33.89	1.40	14.99	161	7.97	32	2.1	17.2	0.07	0.00	181
352	46.64	33.65	1.80	28.17	181	7.51	62	0.0	0.0	0.67	0.18	195
353	46.72	33.25	5.14	32.42	195	7.94	97	0.0	0.0	0.77	0.35	207
354	46.80	33.04	4.36	31.77	207	8.70	104	0.0	0.0	0.28	0.45	218
355	46.89	33.11	4.52	22.89	218	9.06	104	0.0	0.0	0.03	0.05	230
356	46.97	33.51	4.27	14.05	230	8.70	113	0.0	0.0	0.03	0.08	211
357	47.05	33.94	4.69	14.45	211	8.58	147	0.0	0.0	0.06	0.01	214
358	47.14	33.87	3.72	19.73	214	8.36	109	0.3	26.0	0.03	0.19	224
359	47.22	33.61	2.84	16.12	224	9.13	257	0.4	26.0	0.01	0.14	247
360	47.30	33.34	2.63	13.23	247	9.57	232	2.8	26.0	0.00	0.00	268
361	47.39	33.25	2.32	10.38	268	9.24	229	3.2	21.4	0.00	0.00	298
362	47.47	33.37	1.80	4.16	298	9.20	211	0.0	0.0	0.00	0.00	0
363	47.55	33.76	1.26	2.05	174	9.84	255	0.0	0.0	0.00	0.00	0
364	47.64	33.85	0.81	9.10	193	10.23	15	2.4	16.2	0.01	0.00	205
365	47.72	33.61	0.80	18.11	205	10.74	31	1.6	13.4	0.02	0.00	223
366	47.80	33.31	0.68	22.12	223	10.61	23	0.0	0.0	0.00	0.00	0
367	47.89	33.18	0.54	25.35	249	10.12	47	0.0	0.0	0.00	0.00	0
368	47.97	33.50	0.88	17.48	273	9.76	47	0.0	0.0	0.00	0.00	0
369	48.05	33.91	0.95	9.25	329	9.58	38	0.0	0.0	0.00	0.00	0
370	48.14	34.08	0.92	2.73	3	9.82	30	0.0	0.0	0.00	0.00	0
371	48.22	33.93	0.94	1.92	135	10.06	49	0.0	0.0	0.00	0.00	0
372	48.30	33.62	0.85	1.09	223	9.99	30	0.0	0.0	0.00	0.00	0
373	48.39	33.36	0.76	2.02	45	9.91	25	0.0	0.0	0.00	0.00	0
374	48.47	33.38	0.70	7.53	37	8.79	32	2.4	16.0	0.00	0.00	46
375	48.55	33.72	1.54	9.43	46	8.53	30	3.6	26.0	0.00	0.00	138
376	48.64	33.83	2.67	6.90	139	8.59	23	1.9	26.0	0.00	0.00	158
377	48.72	33.70	2.54	9.81	158	9.32	9	2.2	26.0	0.01	0.00	182
378	48.80	33.41	2.25	14.48	182	9.41	14	0.0	0.0	0.03	0.02	205
379	48.89	33.15	3.02	15.29	205	9.18	17	0.0	0.0	0.00	0.02	220
380	48.97	33.19	3.11	6.87	220	10.58	18	0.0	0.0	0.00	0.02	236
381	49.05	33.55	3.48	4.84	236	10.58	27	0.0	0.0	0.00	0.03	188
382	49.14	33.92	3.40	6.24	188	10.82	33	0.0	0.0	0.01	0.03	183
383	49.22	33.95	3.38	9.62	183	10.07	26	0.0	0.0	0.04	0.06	190
384	49.30	33.71	3.25	14.78	189	10.02	35	0.0	0.0	0.08	0.14	207
385	49.39	33.30	3.14	17.50	207	10.48	35	0.0	0.0	0.01	0.01	239
386	49.47	33.14	2.53	11.52	239	10.60	36	0.7	26.0	0.01	0.12	262
387	49.55	33.40	2.38	10.81	262	10.39	48	0.0	0.0	0.00	0.00	240
388	49.64	33.72	2.82	6.19	240	10.20	60	0.0	0.0	0.00	0.01	221
389	49.72	33.82	2.74	6.84	221	10.73	67	1.3	26.0	0.00	0.16	225
390	49.80	33.65	2.19	9.94	225	10.82	63	2.2	26.0	0.01	0.00	228
391	49.89	33.33	1.88	13.20	228	11.07	71	4.1	27.6	0.00	0.00	267
392	49.97	33.24	1.68	8.84	267	10.87	57	3.2	21.3	0.00	0.00	304
393	50.05	33.51	1.47	6.10	303	10.45	57	4.1	27.6	0.00	0.00	353
394	50.14	33.94	1.88	7.68	353	10.35	52	3.3	21.8	0.00	0.00	160
395	50.22	34.18	1.59	1.80	160	10.30	57	3.7	24.6	0.00	0.00	169

cont'd

Burst	Day	Depth	$H_s$	$U$	$\phi_U$	$T_w$	$\phi_e$	$\eta$	$\lambda_b$	$Q_b$	$Q_s$	$Q_{s_{int}}$
		[m]	[m]	[cm/s]	[deg]	[s]	[deg]	[cm]	[cm]	[g s <sup>-1</sup> ]	[g s <sup>-1</sup> ]	[deg]
396	50.30	34.00	1.65	8.03	169	10.42	38	2.8	18.4	0.00	0.00	199
397	50.39	33.58	1.19	9.47	199	10.50	50	3.1	20.7	0.00	0.00	218
398	50.47	33.28	1.35	8.43	218	10.24	52	0.0	0.0	0.00	0.00	0
399	50.55	33.34	1.01	6.46	246	9.71	51	0.0	0.0	0.00	0.00	0
400	50.64	33.70	0.95	4.85	263	10.18	57	0.0	0.0	0.00	0.00	0
401	50.72	33.97	0.79	3.89	213	9.40	70	0.0	0.0	0.00	0.00	0
402	50.80	33.88	0.81	6.46	194	9.52	46	0.0	0.0	0.00	0.00	0
403	50.89	33.50	0.33	7.76	207	9.23	62	0.0	0.0	0.00	0.00	0
404	50.97	33.21	0.51	4.23	232	9.74	43	0.0	0.0	0.00	0.00	0
405	51.05	33.30	0.64	10.62	359	9.50	31	0.0	0.0	0.00	0.00	0
406	51.14	33.69	0.76	17.09	42	9.58	56	0.0	0.0	0.00	0.00	0
407	51.22	34.07	0.48	21.22	67	9.27	59	0.0	0.0	0.00	0.00	0
408	51.30	34.06	1.01	18.04	110	9.21	26	0.0	0.0	0.00	0.00	0
409	51.39	33.67	0.41	21.85	154	8.71	20	2.4	16.1	0.01	0.00	186
410	51.47	33.22	1.21	17.22	186	8.53	340	0.0	0.0	0.00	0.00	0
411	51.55	33.12	1.30	14.56	212	8.03	67	0.0	0.0	0.00	0.00	0
412	51.64	33.44	1.43	12.30	237	8.12	71	0.0	0.0	0.00	0.00	0
413	51.72	33.86	0.97	15.20	230	8.47	270	2.7	17.9	0.03	0.00	224
414	51.80	33.92	1.09	22.56	224	8.93	86	1.8	14.7	0.03	0.00	238
415	51.89	33.59	0.94	23.57	238	8.77	80	3.0	19.7	0.03	0.00	249
416	51.97	33.22	1.10	21.98	249	8.90	69	0.0	0.0	0.00	0.00	0
417	52.05	33.13	1.09	16.84	279	8.29	282	3.0	20.3	0.01	0.00	340
418	52.14	33.49	1.60	15.62	340	8.58	19	2.5	16.9	0.01	0.00	22
419	52.22	34.02	1.40	15.66	22	8.44	46	0.0	0.0	0.00	0.00	0
420	52.30	34.17	1.48	7.77	84	8.74	57	0.0	0.0	0.00	0.00	0
421	52.39	33.81	1.35	9.77	145	9.36	43	2.5	17.0	0.00	0.00	185
422	52.47	33.32	1.50	8.70	185	8.85	46	0.0	0.0	0.00	0.00	0
423	52.55	33.08	1.26	7.85	212	8.77	51	0.0	0.0	0.00	0.00	0
424	52.64	33.30	1.44	5.34	236	8.75	47	0.0	0.0	0.00	0.00	0
425	52.72	33.84	1.32	4.34	215	9.09	32	0.0	0.0	0.00	0.00	0
426	52.80	34.09	1.27	8.35	205	8.86	35	2.4	15.8	0.00	0.00	214
427	52.89	33.79	1.09	14.48	214	9.43	17	3.1	20.7	0.02	0.00	238
428	52.97	33.31	1.22	18.86	238	9.27	40	2.0	26.0	0.03	0.00	254
429	53.05	33.11	2.42	17.93	254	8.82	58	2.2	26.0	0.00	0.00	283
430	53.14	33.29	2.70	6.72	283	8.89	88	1.0	26.0	0.00	0.00	0
431	53.22	33.85	3.20	7.37	4	8.83	80	2.2	26.0	0.00	0.00	80
432	53.30	34.15	2.95	4.69	80	8.77	74	0.0	0.0	0.00	0.01	145
433	53.39	33.91	3.77	9.04	145	8.63	89	0.0	0.0	0.01	0.02	169
434	53.47	33.39	3.70	11.94	169	9.07	83	0.0	0.0	0.03	0.03	166
435	53.55	33.04	3.48	15.67	166	8.88	112	0.0	0.0	0.05	0.07	164
436	53.64	33.10	3.96	16.46	164	8.90	98	0.0	0.0	0.02	0.05	160
437	53.72	33.59	4.18	12.26	160	8.88	97	0.0	0.0	0.06	0.26	167
438	53.80	34.00	3.08	19.06	167	9.23	89	1.7	26.0	0.29	1.19	195
439	53.89	33.85	2.23	30.87	195	9.39	80	4.2	27.7	0.12	0.00	223
440	53.97	33.36	1.61	27.22	223	9.13	81	3.8	25.2	0.06	0.00	247
441	54.05	33.02	1.42	23.86	247	9.03	72	3.0	19.7	0.01	0.00	293
442	54.14	33.19	1.32	16.01	293	9.30	69	0.0	0.0	0.00	0.00	0
443	54.22	33.74	1.08	16.83	348	8.66	57	0.0	0.0	0.00	0.00	0

cont'd

Burst	Day	Depth	$H_s$	$U$	$\phi_U$	$T_w$	$\phi_e$	$\eta$	$\lambda_b$	$Q_b$	$Q_s$	$Q_{s_{int}}$
		[m]	[m]	[cm/s]	[deg]	[s]	[deg]	[cm]	[cm]	[g s <sup>-1</sup> ]	[g s <sup>-1</sup> ]	[deg]
444	54.30	34.19</										

Burst Day	Depth	$H_s$	$U$	$\phi_U$	$T_w$	$\phi_s$	$\eta_b$	$\lambda_b$	$Q_b$	$Q_s$	$Q_{s_{max}}$	
	[m]	[m]	[cm/s]	[deg]	[s]	[deg]	[cm]	[cm]	[g s m <sup>-1</sup> ]	[g s m <sup>-1</sup> ]	[deg]	
540	62.30	33.16	0.61	5.01	189	11.89	342	0.0	0.0	0.00	0	
541	62.39	33.27	0.65	3.65	199	11.68	9	0.0	0.0	0.00	0	
542	62.47	33.65	0.71	5.39	179	11.36	348	0.0	0.0	0.00	0	
543	62.55	33.86	0.69	11.28	192	11.54	357	0.0	0.0	0.00	0	
544	62.64	33.67	0.62	17.80	212	11.79	1	2.0	16.8	0.05	0.00	233
545	62.72	33.36	0.80	25.15	233	11.00	278	0.0	0.0	0.00	0	
546	62.80	33.16	0.65	19.67	251	10.80	285	0.0	0.0	0.00	0	
547	62.89	33.22	0.64	15.16	299	10.46	332	0.0	0.0	0.00	0	
548	62.97	33.67	0.53	11.04	358	10.64	1	0.0	0.0	0.00	0	
549	63.05	34.02	0.54	11.06	36	10.67	18	0.0	0.0	0.00	0	
550	63.14	33.95	0.62	6.87	124	9.73	304	0.0	0.0	0.00	0	
551	63.22	33.62	0.59	10.73	157	11.21	331	0.0	0.0	0.00	0	
552	63.30	33.23	0.47	13.62	186	9.92	333	0.0	0.0	0.00	0	
553	63.39	33.13	0.53	15.83	207	8.18	160	3.3	21.8	0.01	0.00	222
554	63.47	33.37	2.38	15.51	222	7.82	153	0.0	0.0	0.00	0	
555	63.55	33.76	1.60	20.75	224	7.68	159	3.4	22.5	0.07	0.00	228
556	63.64	33.77	2.11	26.34	228	8.01	152	0.0	0.0	0.00	0	
557	63.72	33.58	0.49	22.71	243	9.04	264	0.0	0.0	0.00	0	
558	63.80	33.27	0.71	22.86	260	9.41	286	0.0	0.0	0.00	0	
559	63.89	33.16	0.51	19.25	289	9.44	280	0.0	0.0	0.00	0	
560	63.97	33.44	0.57	13.92	347	10.96	185	0.0	0.0	0.00	0	
561	64.05	33.91	0.63	18.93	19	11.34	196	0.0	0.0	0.00	0	
562	64.14	34.11	0.55	13.26	68	11.38	232	0.0	0.0	0.00	0	
563	64.22	33.89	0.62	9.89	123	12.01	87	0.0	0.0	0.00	0	
564	64.30	33.49	0.52	12.96	154	11.02	324	0.0	0.0	0.00	0	
565	64.39	33.13	0.74	11.23	176	11.20	330	0.0	0.0	0.00	0	
566	64.47	33.21	0.71	7.50	198	11.26	305	0.0	0.0	0.00	0	
567	64.55	33.57	0.77	6.12	200	11.14	306	0.0	0.0	0.00	0	
568	64.64	33.86	0.73	12.48	199	11.54	311	0.0	0.0	0.00	0	
569	64.72	33.77	0.63	16.70	208	10.92	305	2.4	16.3	0.02	0.00	233
570	64.80	33.43	0.76	22.06	233	11.09	290	3.0	20.3	0.04	0.00	255
571	64.89	33.11	0.81	23.23	255	12.80	290	2.5	16.6	0.02	0.00	305
572	64.97	33.10	0.75	19.41	305	11.13	287	2.2	14.6	0.01	0.00	357
573	65.05	33.63	0.75	16.55	357	11.53	359	2.2	14.7	0.01	0.00	27
574	65.14	34.09	0.85	16.52	27	10.70	4	0.0	0.0	0.00	0	
575	65.22	34.15	0.50	6.59	77	9.45	85	2.5	26.0	0.00	0.00	164
576	65.30	33.77	2.88	3.73	164	8.72	290	0.0	0.0	0.01	0.00	237
577	65.39	33.31	3.34	5.90	237	9.72	310	0.0	0.0	0.11	0.00	267
578	65.47	33.07	4.31	9.88	267	9.36	286	0.0	0.0	0.02	0.14	304
579	65.55	33.43	4.15	11.67	305	9.51	312	0.0	0.0	0.02	0.17	320
580	65.64	33.94	4.42	10.83	320	9.61	307	0.0	0.0	0.06	1.73	270
581	65.72	34.11	5.27	12.77	270	10.51	300	0.0	0.0	0.38	1.69	263
582	65.80	33.83	4.48	21.80	263	10.45	310	0.0	0.0	1.32	12.16	266
583	65.89	33.33	5.20	25.84	266	11.20	313	0.0	0.0	1.09	12.29	296
584	65.97	33.07	5.31	24.28	296	10.85	317	0.0	0.0	0.79	9.79	326
585	66.05	33.35	5.21	22.52	325	11.00	322	0.0	0.0	0.50	3.10	359
586	66.14	33.95	4.74	22.22	359	10.65	319	0.0	0.0	0.06	1.06	10
587	66.22	34.35	4.43	13.44	10	11.51	322	0.0	0.0	0.01	0.01	182

cont'd

Burst Day	Depth	$H_s$	$U$	$\phi_U$	$T_w$	$\phi_s$	$\eta_b$	$\lambda_b$	$Q_b$	$Q_s$	$Q_{s_{max}}$	
	[m]	[m]	[cm/s]	[deg]	[s]	[deg]	[cm]	[cm]	[g s m <sup>-1</sup> ]	[g s m <sup>-1</sup> ]	[deg]	
636	70.30	34.00	4.34	3.96	118	11.62	43	0.0	0.0	0.05	0.92	161
637	70.39	34.27	4.59	12.89	161	11.21	54	0.0	0.0	0.38	1.02	170
638	70.47	33.73	3.81	22.83	170	11.37	53	0.0	0.0	0.06	0.16	198
639	70.55	33.04	3.24	15.68	198	10.78	45	0.0	0.0	0.01	0.03	229
640	70.64	32.70	3.07	9.34	229	10.51	49	0.0	0.0	0.00	0.00	277
641	70.72	33.05	2.87	5.79	277	9.70	66	0.0	0.0	0.00	0.00	11
642	70.80	33.90	2.78	2.43	11	10.53	50	1.9	26.0	0.00	0.00	174
643	70.89	34.28	2.37	8.81	174	10.12	49	1.6	26.0	0.04	0.52	187
644	70.97	33.88	2.10	18.28	187	10.30	47	2.8	26.0	0.05	0.00	208
645	71.05	33.20	1.86	19.85	208	9.79	60	2.3	26.0	0.04	0.00	252
646	71.14	32.82	1.96	18.75	252	9.70	62	3.0	20.4	0.01	0.00	296
647	71.22	32.99	1.51	15.87	296	9.10	52	3.2	21.7	0.00	0.00	346
648	71.30	33.74	1.73	10.83	346	9.09	42	0.0	0.0	0.00	0.00	0
649	71.39	34.26	1.39	4.46	143	9.65	42	4.0	26.5	0.02	0.00	173
650	71.47	33.98	1.61	17.47	173	9.90	20	3.6	26.0	0.06	0.00	198
651	71.55	33.30	1.64	22.62	198	9.70	50	4.0	26.3	0.01	0.00	225
652	71.64	32.85	1.70	14.77	225	9.43	64	3.3	22.0	0.00	0.00	274
653	71.72	32.91	1.48	12.61	274	9.37	74	3.9	25.9	0.00	0.00	333
654	71.80	33.59	1.96	9.18	333	9.59	51	3.8	25.1	0.00	0.00	194
655	71.89	34.24	1.79	2.97	194	10.29	59	3.2	21.1	0.00	0.00	182
656	71.97	34.18	1.42	9.85	182	10.54	64	3.8	25.6	0.00	0.00	193
657	72.05	33.54	1.64	11.63	193	10.22	54	3.8	25.1	0.00	0.00	226
658	72.14	32.99	1.64	9.19	226	10.01	64	3.1	20.4	0.00	0.00	265
659	72.22	32.90	1.58	8.59	265	9.01	73	3.2	21.6	0.00	0.00	334
660	72.30	33.41	1.60	7.40	334	9.95	61	0.0	0.0	0.00	0.00	0
661	72.39	34.05	0.97	1.11	163	9.97	73	0.0	0.0	0.00	0.00	0
662	72.47	34.11	1.25	12.37	173	9.53	68	0.0	0.0	0.00	0.00	0
663	72.55	33.56	0.94	14.76	192	9.99	61	2.5	16.6	0.01	0.00	213
664	72.64	33.09	0.95	17.53	213	9.74	55	0.0	0.0	0.00	0.00	0
665	72.72	32.96	0.65	16.18	263	9.81	69	0.0	0.0	0.00	0.00	0
666	72.80	33.37	0.91	13.88	329	9.42	33	0.0	0.0	0.00	0.00	0
667	72.89	34.05	0.80	8.94	15	9.27	35	0.0	0.0	0.00	0.00	0
668	72.97	34.25	0.65	5.45	114	8.87	39	0.0	0.0	0.00	0.00	0
669	73.05	33.82	0.63	9.05	175	7.88	345	2.3	15.2	0.00	0.00	202
670	73.14	33.24	2.15	9.18	202	7.48	0	3.6	24.3	0.00	0.00	233
671	73.22	32.96	2.86	2.69	233	7.74	14	3.3	21.8	0.00	0.00	20
672	73.30	33.20	2.34	4.39	21	8.04	6	3.5	23.1	0.00	0.00	60
673	73.39	33.72	2.21	8.35	60	8.32	34	0.6	26.0	0.01	0.11	139
674	73.47	34.04	2.70	10.88	139	10.03	42	0.0	0.0	0.04	0.04	172
675	73.55	33.62	2.88	15.69	172	10.64	44	0.0	0.0	0.09	0.19	182
676	73.64	33.24	3.37	17.23	182	10.45	37	0.0	0.0	0.00	0.04	203
677	73.72	32.94	3.06	8.85	203	11.16	52	0.0	0.0	0.00	0.01	244
678	73.80	33.14	3.02	6.41	244	10.45	45	0.0	0.0	0.00	0.00	321
679	73.89	33.69	3.08	4.91	321	10.34	46	0.0	0.0	0.00	0.02	191
680	73.97	34.11	3.37	5.26	191	10.68	43	0.0	0.0	0.01	0.01	182
681	74.05	33.92	2.77	8.85	182	10.59	43	1.6	26.0	0.00	0.18	195
682	74.14	33.41	2.20	8.77	195	10.53	35	1.2	26.0	0.00	0.10	202
683	74.22	33.09	2.28	7.84	202	10.49	38	2.6	26.0	0.00	0.00	203

cont'd

Burst Day	Depth	$H_s$	$U$	$\phi_U$	$T_w$	$\phi_s$	$\eta_b$	$\lambda_b$	$Q_b$	$Q_s$	$Q_{s_{max}}$	
	[m]	[m]	[cm/s]	[deg]	[s]	[deg]	[cm]	[cm]	[g s m <sup>-1</sup> ]	[g s m <sup>-1</sup> ]	[deg]	
588	66.30	34.18	4.85	1.04	182	10.77	310	0.0	0.0	0.01	1.49	226
589	66.39	33.57	5.30	7.94	226	11.52	299	0.0	0.0	0.02	0.56	248
590	66.47	33.09	4.49									

Burst Day	Depth	$H_s$	$U$	$\phi_U$	$T_w$	$\phi_c$	$\eta_b$	$\lambda_b$	$Q_b$	$Q_s$	$Q_{s,c}$
[m]	[m]	[cm/s]	[deg]	[s]	[deg]	[cm]	[cm]	[g s m <sup>-1</sup> ]	[g s m <sup>-1</sup> ]	[deg]	
732	78.30	33.54	0.34	7.81	156	9.81	12	0.0	0.0	0.0	0
733	78.39	33.26	0.17	10.63	180	9.38	4	0.0	0.0	0.0	0
734	78.47	33.23	0.33	8.86	209	9.29	48	0.0	0.0	0.0	0
735	78.55	33.52	0.27	7.25	223	9.45	272	0.0	0.0	0.0	0
736	78.64	33.80	0.11	9.19	212	9.52	59	0.0	0.0	0.0	0
737	78.72	33.82	0.22	12.46	216	9.77	280	0.0	0.0	0.0	0
738	78.80	33.62	0.31	11.75	227	9.23	86	0.0	0.0	0.0	0
739	78.89	33.30	0.16	14.79	254	9.87	79	0.0	0.0	0.0	0
740	78.97	33.25	0.23	13.52	287	9.00	284	0.0	0.0	0.0	0
741	79.05	33.53	0.31	9.89	337	10.08	200	0.0	0.0	0.0	0
742	79.14	33.89	0.11	8.63	13	8.35	211	0.0	0.0	0.0	0
743	79.22	33.99	0.25	3.99	94	8.16	229	0.0	0.0	0.0	0
744	79.30	33.78	0.20	10.00	154	8.32	172	0.0	0.0	0.0	0
745	79.39	33.40	0.47	10.78	178	10.14	181	0.0	0.0	0.0	0
746	79.47	33.21	0.32	8.99	195	10.99	208	0.0	0.0	0.0	0
747	79.55	33.40	0.44	4.66	205	9.78	241	0.0	0.0	0.0	0
748	79.64	33.76	0.47	5.79	183	10.64	279	0.0	0.0	0.0	0
749	79.72	33.93	0.53	9.57	177	11.95	320	0.0	0.0	0.0	0
750	79.80	33.78	0.50	12.94	194	11.00	294	0.0	0.0	0.0	0
751	79.89	33.41	0.61	12.28	208	10.69	288	0.0	0.0	0.0	0
752	79.97	33.23	0.42	12.77	260	11.16	276	0.0	0.0	0.0	0
753	80.05	33.39	0.29	10.01	321	10.96	21	0.0	0.0	0.0	0
754	80.14	33.81	0.69	11.27	11	11.43	48	0.0	0.0	0.0	0
755	80.22	34.08	0.63	6.83	69	11.27	68	0.0	0.0	0.0	0
756	80.30	33.97	0.42	8.45	133	12.51	325	0.0	0.0	0.0	0
757	80.39	33.57	0.56	9.02	166	11.39	331	0.0	0.0	0.0	0

Table B-4: Boundary layer parameters output from SEDTRANS96 for S4 input

Day	$u_b$	$A_b$	$f_{cws}$	$u_{cs}$	$u_{ws}$	$u_{cws}$	$u_{cws}$	$u_{cws}$	$u_{cs}$	$u_{ws}$	$u_{cws}$	$\delta_{cw}$	$z_0$	$z_{0c}$
[m]	[m]	(x 100)	[cm/s]	[cm/s]	[cm/s]	[cm/s]	[cm/s]	[cm/s]	[cm/s]	[cm/s]	[cm/s]	[cm]	[cm]	[cm]
17.50	0.22	0.29	1.24	1.8	2.2	2.8	3.6	5.0	3.1	4.9	5.8	6.1	0.2	1.0
17.58	0.28	0.39	1.25	1.0	2.4	2.6	3.6	4.7	1.8	5.7	6.0	6.8	0.2	2.6
17.67	0.23	0.33	1.37	0.9	2.0	2.0	3.8	3.2	1.6	5.8	5.9	6.7	0.4	3.1
18.08	0.24	0.32	1.32	0.9	2.1	2.3	4.0	4.0	1.7	6.0	6.3	6.8	0.4	3.2
18.17	0.25	0.35	1.35	0.9	2.1	2.1	3.9	3.5	1.7	6.2	6.3	7.1	0.5	3.4
18.25	0.12	0.16	1.62	0.9	1.3	1.4	1.4	1.4	0.9	1.3	1.4	1.5	0.0	0.0
18.33	0.27	0.34	1.35	0.7	2.3	2.4	3.7	4.3	1.2	6.2	6.3	6.3	0.3	3.6
18.42	0.17	0.20	1.63	0.3	1.5	1.5	1.5	1.5	0.3	1.5	1.5	1.5	0.0	0.4
18.50	0.18	0.22	1.51	1.0	1.7	1.8	3.4	2.6	1.8	4.9	5.0	4.9	0.4	1.9
18.58	0.13	0.16	1.62	0.8	1.4	1.6	1.6	1.6	0.8	1.4	1.6	1.5	0.0	0.1
18.67	0.13	0.17	1.68	0.5	1.3	1.3	1.3	1.3	0.5	1.3	1.3	1.4	0.0	0.1

cont'd

Day	$u_b$	$A_b$	$f_{cws}$	$u_{cs}$	$u_{ws}$	$u_{cws}$	$u_{cws}$	$u_{cws}$	$u_{cs}$	$u_{ws}$	$u_{cws}$	$\delta_{cw}$	$z_0$	$z_{0c}$
[m]	[m]	(x 100)	[cm/s]	[cm/s]	[cm/s]	[cm/s]	[cm/s]	[cm/s]	[cm/s]	[cm/s]	[cm/s]	[cm]	[cm]	[cm]
18.75	0.19	0.26	1.49	0.7	1.7	1.7	3.2	2.3	1.2	4.7	4.7	5.1	0.3	2.6
18.83	0.17	0.23	1.56	0.2	1.6	1.6	1.6	1.6	0.2	1.6	1.6	1.6	0.0	0.7
18.92	0.15	0.19	1.54	1.0	1.4	1.6	3.0	1.7	1.7	3.7	3.9	4.1	0.3	1.2
19.00	0.15	0.18	1.31	1.9	1.7	2.6	4.1	4.3	3.7	4.5	5.8	5.8	0.4	1.0
19.08	0.16	0.21	1.25	2.1	1.8	2.7	3.9	4.5	3.8	4.4	5.7	6.2	0.3	0.8
19.17	0.13	0.17	1.34	1.7	1.5	2.3	3.6	3.5	3.1	3.8	4.9	5.2	0.3	0.9
19.25	0.12	0.18	1.27	1.8	1.5	2.3	3.6	3.5	3.3	3.6	4.8	5.9	0.3	0.8
19.33	0.10	0.16	1.34	1.6	1.3	2.0	3.2	2.9	2.8	3.1	4.1	4.9	0.3	0.7
19.42	0.11	0.16	1.38	1.4	1.3	1.9	3.0	2.7	2.4	3.1	3.9	4.6	0.2	0.7
20.25	0.11	0.14	1.52	1.3	1.3	1.7	2.8	2.2	2.1	2.9	3.5	3.6	0.2	0.6
20.33	0.14	0.21	1.37	1.4	1.5	1.9	3.0	2.7	2.4	2.5	4.0	4.8	0.2	0.8
20.42	0.37	0.56	1.12	1.3	3.0	3.2	3.2	6.3	2.0	6.0	6.3	7.7	0.1	2.2
20.50	0.49	0.79	1.06	0.3	3.5	3.6	3.6	7.6	0.4	7.6	7.6	9.8	0.2	7.8
20.58	0.45	0.71	1.08	1.0	3.4	3.5	3.5	7.2	1.7	7.1	7.2	9.2	0.2	3.7
20.67	0.37	0.57	1.15	0.9	2.9	3.0	3.2	5.8	1.4	5.8	5.9	7.3	0.1	2.8
20.75	0.37	0.59	1.15	0.3	2.8	2.8	3.2	5.5	0.5	5.8	5.8	7.4	0.1	5.4
20.83	0.35	0.55	1.17	0.8	2.8	2.8	3.2	5.4	1.3	5.8	5.8	7.2	0.1	3.1
20.92	0.30	0.44	1.24	1.4	2.5	2.5	3.5	4.7	2.5	6.0	6.0	7.0	0.2	1.8
21.00	0.34	0.51	1.10	2.2	3.0	3.5	3.5	6.8	3.7	6.2	6.8	8.1	0.2	1.0
21.08	0.30	0.45	1.01	3.3	3.0	4.4	4.4	8.8	5.9	6.7	8.8	10.6	0.3	0.9
21.17	0.29	0.45	1.01	3.1	3.0	4.3	4.3	8.4	5.5	6.4	8.4	10.6	0.2	0.9
21.25	0.23	0.37	1.15	1.9	2.3	2.9	3.5	5.2	3.1	4.8	5.7	7.2	0.2	1.0
21.33	0.18	0.28	1.41	1.0	1.6	1.7	3.2	2.2	1.9	4.3	4.4	5.5	0.3	1.6
21.42	0.15	0.21	1.37	1.3	1.6	2.0	3.8	3.0	2.5	4.4	5.0	5.8	0.4	1.6
21.50	0.35	0.46	1.24	0.3	2.7	2.8	3.2	5.4	0.4	5.9	5.9	6.2	0.1	4.8
21.58	0.33	0.39	1.24	1.3	2.9	3.2	3.2	6.3	2.1	6.0	6.3	6.0	0.1	1.7
21.67	0.46	0.59	1.06	2.3	3.9	4.5	4.5	9.8	4.1	8.9	8.9	10.0	0.3	2.2
21.75	0.50	0.67	1.08	1.2	3.8	4.0	4.0	8.8	2.0	8.6	8.8	9.5	0.2	4.0
21.83	0.46	0.63	1.12	0.8	3.5	3.6	3.6	7.6	1.2	7.6	7.6	8.4	0.2	4.6
21.92	0.60	0.78	1.04	1.9	4.5	4.7	4.7	10.8	3.5	10.6	10.8	11.3	0.3	3.5
22.00	0.77	1.23	0.92	2.5	5.4	5.5	5.5	13.3	5.0	13.0	13.3	16.9	0.4	4.1
22.08	1.31	2.65	0.74	3.4	8.4	8.9	8.9	23.3	8.2	22.3	23.3	37.7	0.8	9.9
22.17	1.05	2.26	0.76	3.3	7.0	7.5	7.5	18.7	7.8	17.6	18.7	32.3	0.6	6.3
22.25	0.96	1.95	0.80	2.1	6.4	6.7	6.7	16.5	4.6	15.9	16.5	26.7	0.5	8.9
22.33	0.88	1.76	0.83	1.6	5.8	6.0	6.0	14.4	3.2	14.1	14.4	23.1	0.4	9.5
22.42	0.92	1.73	0.84	1.9	6.1	6.3	6.3	15.4	4.0	15.0	15.4	23.3	0.5	8.5
22.50	0.68	1.16	0.93	1.2	4.8	4.9	4.9	11.3	2.3	11.1	11.3	15.5	0.3	7.0
22.58	0.66	1.17	0.94	0.9	4.6	4.7	4.7	10.6	1.7	10.5	10.6	15.1	0.3	8.2
22.67	0.63	1.12	0.95	1.2	4.5	4.6	4.6	10.3	2.2	10.1	10.3	14.5	0.3	6.2
22.75	0.54	0.90	1.01	0.9	3.9	4.0	4.0	8.7	1.6	8.6	8.7	11.7	0.2	5.6
22.83	0.58	1.04	0.97	1.1	4.1	4.1	4.1	9.0	1.9	8.9	9.0	13.0	0.2	5.6
22.92	0.42	0.71	1.08	0.6	3.1	3.2	3.2	6.4	0.9	6.3	6.4	8.7	0.1	4.9

cont'd

Day	$u_b$	$A_b$	$f_{cws}$	$u_{cs}$	$u_{ws}$	$u_{cws}$	$u_{cws}$	$u_{cws}$	$u_{cs}$	$u_{ws}$	$u_{cws}$	$\delta_{cw}$	$z_0$	$z_{0c}$
[m]	[m]	(x 100)	[cm/s]	[cm/s]	[cm/s]	[cm/s]	[cm/s]	[cm/s]	[cm/s]	[cm/s]	[cm/s]	[cm]	[cm]	[cm]
23.00	0.36	0.61	1.10	1.4	2.8	3.0	3.2	5.8	2.2	5.7	5.9	8.0	0.1	1.7
23.08	0.34	0.56	1.11	2.2	2.8	3.1	3.2	6.0	3.7	5.7	6.0	7.7	0.1	0.7
23.17	0.34	0.54	0.97	3.6	3.4	4.8	4.8	9.9	7.0	7.6	9.9	12.6	0.3	0.9
23.25	0.30	0.46	1.03	3.0	2.9	4.1	4.1	8.1	5.4	6.3	8.1	10.1	0.2	0.8
23.33	0.22	0.35	1.16	1.8	2.2	2.8	3.6	5.1	3.2	4.7	5.7	7.3	0.2	1.0
23.42	0.25	0.38	1.22	1.5	2.2	2.5	3.8	4.5	2.8	5.5	6.0	7.3	0.3	1.6
23.50	0.21	0.33	1.34	1.1	1.8	1.9	3.6	2.9	2.2	5.1	5.2	6.6	0.4	2.0
23.58	0.15	0.22	1.57	0.3	1.4	1.4	1.4	1.4	0.3	1.4	1.4	1.6	0.0	0.4
23														

Day	$u_b$	$A_b$	$f_{cws}$	$u_{+cs}$	$u_{+ws}$	$u_{+cws}$	$u_{+cws}$	$u_{+cwb}$	$u_{+c}$	$u_{+w}$	$u_{+cw}$	$\delta_{cw}$	$z_0$	$z_{0c}$
	[cm/s]	[m]	(x 100)	[cm/s]	[cm/s]	[cm/s]	[cm/s]	[cm/s]	[cm/s]	[cm/s]	[cm/s]	[cm]	[cm]	[cm]
30.83	0.24	0.31	1.41	0.4	2.1	2.1	4.0	3.6	0.6	6.4	6.4	6.5	0.5	5.1
30.92	0.20	0.26	1.47	0.5	1.8	1.8	3.5	2.8	0.9	5.2	5.3	5.5	0.4	3.5
31.00	0.18	0.23	1.53	0.6	1.6	1.6	3.1	1.9	1.1	4.3	4.3	4.6	0.3	2.3
31.08	0.09	0.12	1.75	0.7	1.0	1.2	1.2	1.2	0.7	1.0	1.2	1.3	0.0	0.0
31.17	0.13	0.16	1.63	0.8	1.3	1.5	1.5	1.5	0.8	1.3	1.5	1.5	0.0	0.1
31.25	0.19	0.23	1.54	0.9	1.7	1.8	3.3	2.5	1.7	5.0	5.0	4.8	0.4	2.0
31.33	0.27	0.33	1.31	1.4	2.4	2.6	3.5	4.8	2.5	5.7	6.0	5.9	0.2	1.5
31.42	0.43	0.53	1.11	2.0	3.6	4.0	4.0	8.7	3.6	8.1	8.7	8.6	0.2	1.9
31.50	0.75	1.11	0.93	2.0	5.4	5.8	5.8	14.0	4.0	13.4	14.0	16.5	0.4	5.7
31.58	0.67	1.08	0.96	1.6	4.8	4.9	4.9	11.3	3.0	11.1	11.3	14.4	0.3	5.1
31.67	0.87	1.50	0.88	1.4	5.9	5.9	5.9	14.5	2.8	14.4	14.5	20.0	0.4	9.5
31.75	0.58	0.98	0.99	1.0	4.2	4.2	4.2	9.3	1.8	9.3	9.3	12.5	0.2	5.8
31.83	0.74	1.31	0.91	2.2	5.1	5.2	5.2	12.1	4.5	11.9	12.1	17.2	0.4	4.1
31.92	0.67	1.16	0.91	2.9	4.9	5.3	5.3	12.3	5.8	11.6	12.3	16.8	0.4	2.8
32.00	0.68	1.24	0.92	2.4	4.8	4.9	4.9	11.1	4.6	10.9	11.1	16.3	0.3	3.2
32.08	0.62	1.09	0.95	1.3	4.4	4.6	4.6	10.2	2.4	10.0	10.2	14.4	0.3	5.7
32.17	0.56	0.96	0.98	1.2	4.1	4.2	4.2	9.3	2.2	9.1	9.3	12.6	0.2	5.0
32.25	0.57	0.97	0.98	1.2	4.1	4.3	4.3	9.4	2.2	9.2	9.4	12.8	0.2	5.0
32.33	0.52	0.92	0.98	1.6	3.9	4.1	4.1	8.7	2.9	8.4	8.7	12.4	0.2	3.4
32.42	0.48	0.84	0.98	1.9	3.7	4.1	4.1	8.7	3.4	8.1	8.7	12.2	0.2	2.6
32.50	0.50	0.88	1.01	1.0	3.7	3.8	3.8	8.1	1.8	8.0	8.1	11.4	0.2	4.7
32.58	0.42	0.74	1.07	0.7	3.1	3.1	3.1	6.3	1.0	6.2	6.3	8.9	0.1	4.5
32.67	0.40	0.68	1.10	0.7	3.0	3.0	3.1	6.0	1.1	5.9	6.0	8.3	0.1	3.9
32.75	0.42	0.70	1.10	0.4	3.1	3.1	3.1	6.4	0.7	6.4	6.4	8.5	0.1	5.5
32.83	0.44	0.73	1.07	1.4	3.3	3.4	3.4	7.1	2.4	7.0	7.1	9.2	0.2	2.4
32.92	0.40	0.62	1.08	2.1	3.2	3.5	3.5	7.2	3.6	6.8	7.2	8.9	0.2	1.2
33.00	0.41	0.64	1.06	1.9	3.3	3.7	3.7	7.6	3.4	7.0	7.6	9.5	0.2	1.7
33.08	0.40	0.65	1.08	1.4	3.2	3.5	3.5	7.0	2.4	6.6	7.0	9.0	0.2	2.3
33.17	0.38	0.61	1.11	0.9	2.9	3.1	3.1	6.1	1.4	5.9	6.1	7.9	0.1	3.1
33.25	0.32	0.48	1.21	0.6	2.5	2.6	3.5	4.9	1.0	5.9	6.0	7.3	0.2	4.0
33.33	0.29	0.45	1.23	0.8	2.4	2.5	3.6	4.6	1.4	5.9	6.1	7.4	0.3	3.6
33.42	0.29	0.44	1.20	1.1	2.5	2.7	3.5	4.9	1.9	5.6	5.9	7.1	0.2	2.3
33.50	0.28	0.43	1.22	0.9	2.4	2.5	3.6	4.6	1.6	5.8	6.0	7.4	0.3	3.0
33.58	0.25	0.37	1.29	0.9	2.1	2.2	4.1	3.9	1.7	6.2	6.4	7.6	0.5	3.6
33.67	0.23	0.35	1.31	1.2	2.0	2.1	4.0	3.4	2.6	5.8	6.0	7.2	0.5	2.2
33.75	0.26	0.40	1.28	0.8	2.1	2.2	4.1	3.8	1.6	6.4	6.5	8.0	0.5	4.1
33.83	0.25	0.36	1.32	0.8	2.1	2.1	4.0	3.6	1.5	6.2	6.3	7.3	0.5	3.9
33.92	0.22	0.32	1.22	1.8	2.1	2.6	3.8	4.6	3.4	5.1	5.9	7.0	0.3	1.1
34.00	0.16	0.23	1.22	2.2	1.9	2.8	3.8	4.7	4.1	4.4	5.7	6.4	0.3	0.6
34.08	0.23	0.31	1.19	2.0	2.3	3.0	3.4	5.5	3.4	4.8	5.8	6.3	0.2	0.7
34.17	0.29	0.35	1.32	1.0	2.5	2.6	3.4	5.0	1.8	5.8	6.0	5.8	0.2	2.1
34.25	0.33	0.39	1.31	0.5	2.7	2.7	3.2	5.3	0.8	5.9	5.9	5.6	0.2	3.4

ccms'd

Day	$u_b$	$A_b$	$f_{cws}$	$u_{+cs}$	$u_{+ws}$	$u_{+cws}$	$u_{+cws}$	$u_{+cwb}$	$u_{+c}$	$u_{+w}$	$u_{+cw}$	$\delta_{cw}$	$z_0$	$z_{0c}$
	[cm/s]	[m]	(x 100)	[cm/s]	[cm/s]	[cm/s]	[cm/s]	[cm/s]	[cm/s]	[cm/s]	[cm/s]	[cm]	[cm]	[cm]
34.33	0.31	0.39	1.31	0.5	2.5	2.6	3.4	4.9	0.8	6.0	6.1	6.0	0.2	3.9
34.42	0.29	0.38	1.30	1.0	2.4	2.5	3.5	4.7	1.7	6.0	6.1	6.3	0.2	2.5
34.50	0.36	0.47	1.20	1.5	2.9	3.1	3.1	6.1	2.4	5.9	6.1	6.5	0.1	1.4
34.58	0.28	0.36	1.34	0.7	2.3	2.3	3.7	4.2	1.3	6.4	6.4	6.7	0.4	3.7
34.67	0.25	0.34	1.37	0.3	2.1	2.1	4.0	3.6	0.5	6.4	6.4	7.0	0.5	5.8
34.75	0.26	0.34	1.36	0.7	2.1	2.2	4.1	3.8	1.4	6.6	6.6	7.0	0.5	4.1
34.83	0.25	0.33	1.36	0.5	2.1	2.2	4.1	3.8	1.0	6.5	6.5	7.0	0.5	4.6
34.92	0.24	0.33	1.23	1.6	2.2	2.7	3.6	4.9	2.9	5.2	5.9	6.5	0.2	1.3
35.00	0.30	0.44	1.09	2.5	2.9	3.7	3.7	7.2	4.3	6.0	7.2	8.4	0.2	0.9